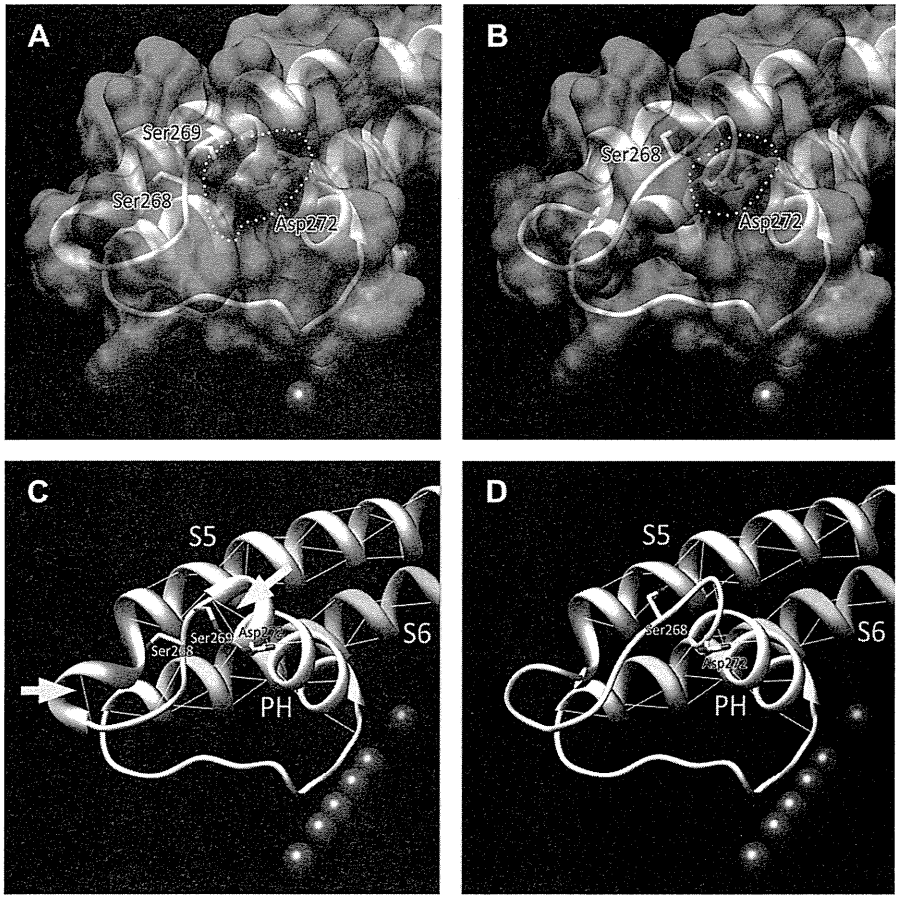

Fig. 3. Partial structural model of KCNQ4 and the p.Ser269del mutation. (A and B) The ribbon models of (A) wild-type KCNQ4 subunit and (B) KCNQ4 subunit with the p.Ser269del mutation overlaid with their corresponding electrostatic surface potential. Red or blue area: negatively or positively charged residues, yellow dot circle: negatively charged surface potential on the N-terminal region of the pore helix (PH). (C and D) Ribbon models of (C) wild-type KCNQ4 and (D) KCNQ4 with the p.Ser269del mutation. Green lines: putative hydrogen bonds; yellow arrows: hydrogen bonds within S5 and PH; purple spheres: potassium ions. (For interpretation of the references to color in this figure legend, the reader is referred to the web version of this article.)

3.3. Predicted structural change in KCNQ4 caused by the p.Ser269del mutation

The ribbon model of the wild-type KCNQ4 subunit overlaid with the corresponding electrostatic surface potential demonstrated that the surface of the N-terminal region of PH is negatively charged because of the negatively charged side chains of Ser269 and Asp272 (Fig. 3A). The model of KCNQ4 with the p.Ser269del mutation demonstrated reduction of the negatively charged surface area in this region (Fig. 3B). Reduction of the electrostatic surface potential in this area has been predicted to impede K+ transport because of the long range electrostatic attractive force between PH and K+ [13]. In addition, hydrogen bonds on the C-terminus of S5 and the N-terminus of PH of wild-type KCNQ4 (Fig. 3C, yellow arrows) were absent in KCNQ4 with the Ser269del mutation (Fig. 3D). Loss of the hydrogen bonds around the N-terminus of PH resulted in shortening of the PH and was attributed to destabilization of α-helix formation [24]. The disrupted helices would affect the structural stability of the pore region and lead to abnormal channel function.

4. Discussion

Most of the *KCNQ4* non-truncating mutations affecting the pore region are associated with severe hearing loss. However, we found that the non-truncating p.Tyr270His [14] and p.Ser269del mutations were associated with moderate hearing loss. *KCNQ4* mutations at or proximal to the N-terminus of PH are suggested to be associated with moderate hearing loss, because this site is predicted to have relatively smaller influence than other pore regions, such as S5, S6, the central region of PH, and the P-loop, on KCNQ4 channel function.

The molecular pathology associated with the p.Ser269del mutation, demonstrated in silico, indicates a reduction in the negatively charged electrostatic surface potential and structural distortion of the pore region by the mutated KCNQ4, which may explain the associated moderate hearing loss. The molecular mechanism in this case is likely to be a mild dominant negative effect resulting from the relatively small influence of *KCNQ4* with the p.Ser269del mutation on the normal channel subunit. However, another possibility is haploinsufficiency resulting from the loss of function of *KCNQ4* with the p.Ser269del mutation. This scenario, which would not affect the functioning of the other channel subunits, cannot be excluded.

5. Conclusion

We found a novel heterozygous *KCNQ4* mutation, c.806_808delCCT (p.Ser269del), in a pedigree with progressive and moderate hearing loss. Molecular modeling analysis of this mutation demonstrated that changes in electrostatic surface potential and structural distortion could be relevant to the pathology underlying

auditory dysfunction. Mutations at or proximal to the N-terminus of the PH of the KCNQ4 channel might cause mild molecular dysfunction and be associated with moderate hearing loss.

Acknowledgment

This study was supported by a Grant-in-Aid for Clinical Research from the National Hospital Organization.

References

[1] <http://hereditaryhearingloss.org/> (accessed September 2012).
[2] C. Kubisch, B.C. Schroeder, T. Friedrich, B. Lütjohann, A. El Amraoui, S. Marlin, C. Petit, T.J. Jentsch, KCNQ4, a novel potassium channel expressed in sensory outer hair cells, is mutated in dominant deafness, Cell 96 (1999) 437–446.
[3] P.J. Coucke, P. Van Hauwe, P.M. Kelley, H. Kunst, I. Schatteman, D. Van Velzen, J. Meyers, R.J. Ensink, M. Verstreken, F. Declau, H. Marres, K. Kastury, S. Bhasin, W.T. McGuirt, R.J. Smith, C.W. Cremers, P. Van de Heyning, P.J. Willems, S.D. Smith, G. Van Camp, Mutations in the KCNQ4 gene are responsible for autosomal dominant deafness in four DFNA2 families, Hum. Mol. Genet. 8 (1999) 1321–1328.
[4] J. Akita, S. Abe, H. Shinkawa, W.J. Kimberling, S. Usami, Clinical and genetic features of nonsyndromic autosomal dominant sensorineural hearing loss: KCNQ4 is a gene responsible in japanese, J. Hum. Genet. 46 (2001) 355–361.
[5] G. Van Camp, P.J. Coucke, J. Akita, E. Fransen, S. Abe, E.M. De Leenheer, P.L. Huygen, C.W. Cremers, S. Usami, A mutational hot spot in the KCNQ4 gene responsible for autosomal dominant hearing impairment, Hum. Mutat. 20 (2002) 15–19.
[6] Z. Talebizadeh, P.M. Kelley, J.W. Askew, K.W. Beisel, S.D. Smith, Novel Mutation in the KCNQ4 Gene in a large kindred with dominant progressive hearing loss, Hum. Mutat. 14 (1999) 493–501.
[7] J. Arnett, S.B. Emery, T.B. Kim, A.K. Boerst, K. Lee, S.M. Leal, M.M. Lesperance, Autosomal dominant progressive sensorineural hearing loss due to a novel mutation in the KCNQ4 gene, Arch. Otolaryngol. Head Neck Surg. 137 (2011) 54–59.
[8] A. Mencía, D. González-Nieto, S. Modamio-Høybjør, A. Etxeberría, G. Aránguez, N. Salvador, I. Del Castillo, A. Villarroel, F. Moreno, L. Barrio, M.A. Moreno-Pelayo, A novel KCNQ4 pore-region mutation (p.G296S) causes deafness by impairing cell-surface channel expression, Hum. Genet. 123 (2008) 41–53.
[9] M.S. Hildebrand, D. Tack, S.J. McMordie, A. DeLuca, I.A. Hur, C. Nishimura, P. Huygen, T.L. Casavant, R.J. Smith, Audioprofile-directed screening identifies novel mutations in KCNQ4 causing hearing loss at the DFNA2 locus, Genet. Med. 10 (2008) 797–804.
[10] J.I. Baek, H.J. Park, K. Park, S.J. Choi, K.Y. Lee, J.H. Yi, T.B. Friedman, D. Drayna, K.S. Shin, U.K. Kim, Pathogenic effects of a novel mutation (c.664_681del) in KCNQ4 channels associated with auditory pathology, Biochim. Biophys. Acta 2011 (1812) 536–543.
[11] F. Kamada, S. Kure, T. Kudo, Y. Suzuki, T. Oshima, A. Ichinohe, K. Kojima, T. Niihori, J. Kanno, Y. Narumi, A. Narisawa, K. Kato, Y. Aoki, K. Ikeda, T. Kobayashi, Y. Matsubara, A novel KCNQ4 one-base deletion in a large pedigree with hearing loss: implication for the genotype-phenotype correlation, J. Hum. Genet. 51 (2006) 455–460.
[12] P. Van Hauwe, P.J. Coucke, R.J. Ensink, P. Huygen, C.W. Cremers, G. Van Camp, Mutations in the KCNQ4 K+ channel gene, responsible for autosomal dominant hearing loss, cluster in the channel pore region, Am. J. Med. Genet. 93 (2000) 184–187.
[13] K. Namba, H. Mutai, H. Kaneko, S. Hashimoto, T. Matsunaga, In silico modeling of the pore region of a KCNQ4 missense mutant from a patient with hearing loss, BMC Res. Notes 5 (2012) 145.
[14] H.J. Kim, P. Lv, C.R. Sihn, E.N. Yamoah, Cellular and molecular mechanisms of autosomal dominant form of progressive hearing loss, DFNA2, J. Biol. Chem. 286 (2011) 1517–1527.
[15] T. Matsunaga, Value of Genetic testing in the ontological approach for sensorineural hearing loss, Keio J. Med. 58 (2009) 216–222.
[16] X. Chen, Q. Wang, F. Ni, J. Ma, Structure of the full-length shaker potassium channel Kv1.2 by normal-mode-based X-ray crystallographic refinement, Proc. Natl. Acad. Sci. USA 107 (2010) 11352–11357.
[17] S.F. Altschul, T.L. Madden, A.A. Schäffer, J. Zhang, Z. Zhang, W. Miller, D.J. Lipman, Gapped BLAST and PSI-BLAST: a new generation of protein database search programs, Nucleic Acids Res. 25 (1997) 3389–3402.
[18] R.A. Laskowski, Enhancing the functional annotation of PDB structures in PDBsum using key figures extracted from the literature, Bioinformatics 23 (2007) 1824–1827.
[19] <http://swissmodel.expasy.org/> (accessed November 2012).
[20] <http://nihserver.mbi.ucla.edu/Verify_3D> (accessed November 2012).
[21] K. Arnold, L. Bordoli, J. Kopp, T. Schwede, The SWISS-MODEL workspace: a web-based environment for protein structure homology modeling, Bioinformatics 22 (2006) 195–201.
[22] E.F. Pettersen, T.D. Goddard, C.C. Huang, G.S. Couch, D.M. Greenblatt, E.C. Meng, T.E. Ferrin, UCSF Chimera – a visualization system for exploratory research and analysis, J. Comput. Chem. 25 (2004) 1605–1612.
[23] <http://evs.gs.washington.edu/EVS/> (accessed August 2012).
[24] W.G. Hol, Effects of the alpha-helix dipole upon the functioning and structure of proteins and peptides, Adv. Biophys. 19 (1985) 133–165.

International Journal of Pediatric Otorhinolaryngology 77 (2013) 228–232

Contents lists available at SciVerse ScienceDirect

International Journal of Pediatric Otorhinolaryngology

journal homepage: www.elsevier.com/locate/ijporl

High prevalence of inner-ear and/or internal auditory canal malformations in children with unilateral sensorineural hearing loss

Sawako Masuda [a,*], Satoko Usui [a], Tatsuo Matsunaga [b]

[a] Department of Otorhinolaryngology, Institute for Clinical Research, National Mie Hospital, Tsu, Mie, Japan
[b] Department of Otolaryngology, Laboratory of Auditory Disorders, National Institute of Sensory Organs, National Tokyo Medical Center, Tokyo, Japan

ARTICLE INFO

Article history:
Received 14 August 2012
Received in revised form 29 October 2012
Accepted 3 November 2012
Available online 30 November 2012

Keywords:
Unilateral sensorineural hearing loss
Temporal bone computed tomography
Malformation
Inner ear
Cochlear nerve canal
Internal auditory canal

ABSTRACT

Objective: Radiological and genetic examination has recently advanced for diagnosis of congenital hearing loss. The aim of this study was to elucidate the prevalence of inner-ear and/or internal auditory canal malformations in children with unilateral sensorineural hearing loss (USNHL) for better management of hearing loss and genetic and lifestyle counseling.
Methods: We conducted a retrospective study of charts and temporal bone computed tomography (CT) findings of 69 consecutive patients 0–15 years old with USNHL. In two cases, genetic examination was conducted.
Results: Of these patients, 66.7% had inner-ear and/or internal auditory canal malformations. The prevalence of malformations in infants (age <1 year) was 84.6%, which was significantly higher than that in children 1–15 years old (55.8%; $p < 0.01$). Almost half of the patients (32; 46.4%) had cochlear nerve canal stenosis; 13 of them had cochlear nerve canal stenosis alone, and in 19 it accompanied other malformations. Internal auditory canal malformations were observed in 22 subjects (31.8%), 14 (20.3%) had cochlear malformations, and 5 (7.2%) had vestibular/semicircular canal malformations. These anomalies were seen only in the affected ear, except in two of five patients with vestibular and/or semicircular canal malformations. Two patients (2.9%) had bilateral enlarged vestibular aqueducts. Mutations were found in *SLC26A4* in one of the two patients with bilateral large vestibular aqueducts. The prevalence of a narrow internal auditory canal was significantly higher in subjects with cochlear nerve canal stenosis (50.0%) than in subjects with normal cochlear nerve canals (11.1%; $p < 0.01$). There were no correlations between the type and number of malformations and hearing level.
Conclusions: The prevalence of inner-ear and/or internal auditory canal malformations detected by high-resolution temporal bone CT in children with USNHL was very high. Radiological and genetic examination provided important information to consider the pathogenesis and management of hearing loss. Temporal bone CT should be recommended to children with USNHL early in life. *SLC26A4* mutation also should be examined in cases with bilateral enlarged vestibular aqueduct.

1. Introduction

Abnormalities of the temporal bone have been associated with congenital sensorineural hearing loss (SNHL) since reported by Mondini in 1791 [1]. However, most cases of congenital SNHL were believed to be caused by abnormalities of the membranous labyrinth that could not be detected by conventional imaging techniques [2,3]. Conventional computed tomography (CT) could identify congenital cochlear malformations such as complete labyrinthine aplasia (Michel deformity), a common cavity, cochlear aplasia/hypoplasia, and incomplete partition [2–4]. Because of improvements in high-resolution CT techniques, previously unrecognized bony abnormalities—including a large vestibular aqueduct, wide and stenotic internal auditory canal (IAC), and cochlear nerve canal (CNC) stenosis—have been reported [3,5]. Currently, abnormalities found by imaging techniques not only provide diagnostic information but also aid in genetic and lifestyle counseling [1] and guide clinicians to better management of hearing loss [6].

The aim of this study was to elucidate the prevalence of inner-ear and/or IAC malformations in children with unilateral SNHL (USNHL).

* Corresponding author at: Department of Otorhinolaryngology, National Mie Hospital, 357 Osato-Kubota, Tsu, Mie 514-0125, Japan. Tel.: +81 59 232 2531; fax: +81 59 232 5994.
E-mail address: masudas@mie-m.hosp.go.jp (S. Masuda).

0165-5876/$ – see front matter © 2012 Elsevier Ireland Ltd. All rights reserved.
http://dx.doi.org/10.1016/j.ijporl.2012.11.001

2. Patients and methods

We conducted a retrospective study of charts and temporal bone CT findings of consecutive USNHL patients 0–15 years old who were seen in the Department of Otorhinolaryngology of National Mie Hospital between January 2008 and December 2011. All procedures were approved by the Ethics Review Committee of National Mie Hospital.

2.1. Subjects

The study included 69 patients. USNHL was defined as a hearing threshold greater than 30 dB hearing level for at least one frequency (500–2000 Hz). Of the 69 patients, 32 were male and 37 were female. Their ages of diagnosis ranged from 0 to 15 years (mean ± 1 SD: 4.3 ± 6.7 years, median: 4 years). The distribution of age was shown in Fig. S1. Twenty-six (37.3% of the subjects) were infants less than 1 year old. Twenty-two children had failed newborn hearing screening (NBHL) in unilateral ear and 21 of them identified USNHL in 1 year of age. One boy who had failed NBHL first visited ENT clinic and diagnosed USNHL at the age of 3 years. There was neither subjects who passed NBHL nor ones who suspected progressive hearing loss before their diagnosis. One subject had Down's syndrome and one had tetralogy of Fallot. Patients with middle ear diseases and abnormalities, conductive and combined hearing loss revealed by pure-tone audiometry, and obvious acquired hearing loss were excluded from the study.

Supplementary material related to this article found, in the online version, at http://dx.doi.org/10.1016/j.ijporl.2012.11.001.

2.2. Audiometric evaluations

Severity of hearing loss was defined from the pure-tone average as follows: hearing level of 21–40 dB, mild; 41–70 dB, moderate; 71–95 dB, severe; and greater than 95 dB, profound [7]. Pure-tone average was defined as the average hearing threshold at 500, 1000, and 2000 Hz. Thirty-four patients in this study were too young to be examined with pure-tone audiometry initially; for these patients, USNHL was determined on the basis of auditory brainstem response (ABR) and auditory steady state response (ASSR) using an Audera® system (Grason-Stadler). Distortion product otoacoustic emissions (DPOAE) and tympanometry were performed for all subjects.

2.3. Evaluation of temporal bone CT findings

All the patients underwent high-resolution CT of temporal bone using a single-slice helical CT (HiSpeed DX/i, GE Healthcare Japan Ltd., Tokyo Hino, Japan). Contiguous 1 mm-thick sections parallel to the infraorbitomeatal line were acquired through the temporal bone, with a field of view of 230 mm, matrix size of 512 × 512, in-plane pixel size of 0.45 mm × 0.45 mm, tube voltage of 120 kV, tube current of 150 mAs and a reconstruction kernel for bone.

CT results for each patient were examined by two otologists who did not know which ear had hearing loss. Classification of inner-ear and IAC malformations was based on Sennaroglu's classification [4] and modified as follows:

1. Cochlear malformations: Michel deformity, cochlear aplasia, common cavity deformity, cochlear hypoplasia, incomplete partition type I (IP-I), incomplete partition type II (IP-II: Mondini deformity).
2. Vestibular/semicircular canal malformations: absent vestibule, hypoplastic vestibule, dilated vestibule/absent semicircular canal, hypoplastic semicircular canal, enlarged semicircular canal.
3. IAC malformations: absent, narrow, enlarged.
4. Vestibular aqueduct finding: large.
5. CNC finding: stenosis.

We defined IAC as narrow when the diameter at the level of the porous of the IAC was less than 3 mm or 2 mm smaller than the normal side and as wide when greater than 10 mm. A large vestibular aqueduct was defined as being greater than 1.5 mm at the midpoint of the vestibular aqueduct on axial images [8]. The width of the CNC was measured at its midportion. The measurements were manually obtained using calipers [5]. CNC stenosis was defined as when the width was less than 1.5 mm [9]. An example of CNC stenosis in the right ear is shown in Fig. 1.

2.4. Genetic examinations

Patients with large vestibular aqueducts participated in genetic examination. Blood samples were obtained from the proband and his/her parents. DNA was extracted from blood samples using the Gentra Puregene DNA isolation kit (Qiagen, Hamburg, Germany), and primers specific for *SLC26A4* (GenBank NG_008489) were designed. Primer sequences for *SLC26A4* are listed in Table S1, supporting information. Screening for *SLC26A4* mutations was performed by bidirectional sequencing of amplicons generated by PCR amplification of each exon (exons 1–21) and splice sites using an Applied Biosystems 3730 DNA Analyzer (Applied Biosystems, Foster City, CA, USA) and analyzed by SeqScape v2.6 (Applied Biosystems). Examinations were conducted only after written informed consent had been obtained from each individual or parents of the patients.

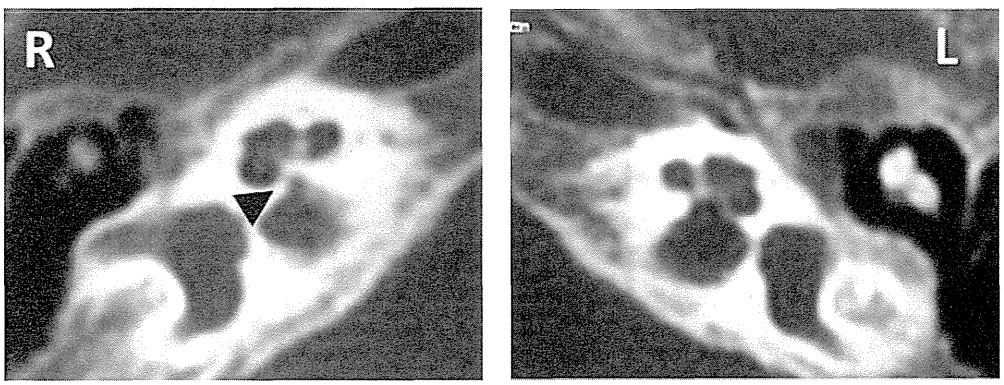

Fig. 1. Cochlear nerve canal stenosis demonstrated by transverse, thin-section CT scan of the temporal bone in three-month old boy. The left panel shows the hearing-impaired right ear (R), and the right panel shows the normal left ear (L). The arrowhead indicates the stenotic cochlear nerve canal in the right ear.

Supplementary material related to this article found, in the online version, at http://dx.doi.org/10.1016/j.ijporl.2012.11.001.

2.5. Statistical analysis

The significance of the prevalence of the inner-ear and/or IAC malformations between infants younger than 1 year of age and children from 1 to 15 years of age, and the association between the existence of malformations and hearing level was determined by the χ^2 test.

3. Results

The prevalence of inner-ear and/or IAC malformations is shown in Fig. 2. Of the 69 subjects, 66.7% had malformations. The prevalence of malformations in infants younger than 1 year of age (84.6%) was significantly higher than that in children 1–15 years of age (55.8%; $p < 0.01$).

Table 1 shows the prevalence of each malformation. The most common anomaly was CNC stenosis of the affected ear, seen in 46.4% of the subjects. Next in frequency were IAC malformations, followed by cochlear malformations and vestibular and/or semicircular canal malformations. These anomalies were seen in the affected ear alone, except for two of five patients with vestibular and/or semicircular canal malformations. Two patients had bilateral enlarged vestibular aqueducts.

The combination of malformations we observed is summarized in Table 2. Of the 69 patients, 13 (18.8%) had CNC stenosis alone, 19 (27.5%) had CNC stenosis accompanied with other malformations, and 4 (5.8%) had narrow IAC alone. Two patients with bilateral enlarged vestibular aqueducts had cochlear or cochlear and vestibular/semicircular canal malformations. In both cases, unilateral hearing loss was found by newborn hearing screening. In one case, a 4-month-old boy, genetic examination identified a compound heterozygous mutation [p.T410M (c.1229C>T)/p.L743X (c.2228T>A)] in *SLC26A4* (Fig. S2). p.T410M was previously reported as a missense mutation [10] and p.L743X was previously reported as a nonsense mutation [11]. This nonsense substitution truncates the protein at codon 743, which is 38 amino acids from the end of the protein. This case was confirmed as Pendred syndrome. The hearing loss in his normal hearing ear developed at 1 year of age. In another case, a 2-month-old girl, pathological mutations were not found in *SLC26A4*. Her hearing level has been stable for 3 years.

Supplementary material related to this article found, in the online version, at http://dx.doi.org/10.1016/j.ijporl.2012.11.001.

Table 3 shows the relationship between CNC malformations and IAC malformations. Of 32 cases of CNC stenosis, 16 (50.0%) were comorbid with narrow IAC. In 36 subjects with normal CNC, 4 (11.1%) had narrow IAC. The prevalence of narrow IAC was significantly higher in subjects with CNC stenosis than in subjects with normal CNC ($p < 0.01$).

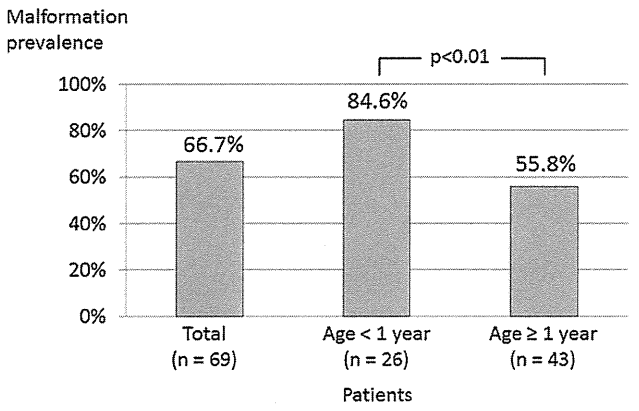

Fig. 2. Prevalence of inner-ear and/or internal auditory canal malformations found by temporal bone computed tomography.

Table 1
Prevalence of each malformation.

Malformation	Number (prevalence)
Cochlea	14 (20.3%)
Cochlear aplasia	0
Common cavity deformity	2 (2.9%)
Cochlear hypoplasia	1 (1.4%)
Incomplete partition (IP-I, IP-II)	11 (15.9%)
Vestibular/semicircular canal	5[a] (7.2%)
Internal auditory canal	22 (31.8%)
Narrow	20 (29.0%)
Enlarged	1 (1.4%)
Absent	1 (1.4%)
Vestibular aqueduct: enlarged (bilateral)	2 (2.9%)
Cochlear nerve canal: stenosis	32 (46.4%)

[a] Two cases had malformation in both ears.

Table 2
Combination of malformations.

Combination of malformations	Number (percentage)
CNC stenosis	13 (18.8)
CNC stenosis + narrow IAC	10 (14.5)
CNC stenosis + narrow IAC + C malformations	5 (7.2)
CNC stenosis + narrow IAC + V/SC malformations	1[a] (1.4)
CNC stenosis + C malformations	3 (4.3)
Narrow IAC	4 (5.8)
Large IAC	1 (1.4)
C malformations	2 (2.9)
C/V/SC malformations	2 (2.9)
V/SC malformations	2[b] (2.9)
Large VA + C malformations	1 (1.4)
Large VA + C malformations + V/SC malformations	1 (1.4)
CC with absent IAC	1 (1.4)
Normal	23 (33.3)
Total	69 (100.0)

CNC stenosis, cochlear nerve canal stenosis; IAC, internal auditory canal; C, Cochlear; V/SC, vestibular/semicircular canal; VA, vestibular aqueduct; CC: common cavity.
[a] This patient had bilateral V/SC malformations.
[b] One patient had bilateral V/SC malformations.

Table 4 shows the combination of malformations and hearing level. There were 6 cases of mild hearing loss, 13 cases of moderate hearing loss, 7 cases of severe hearing loss, and 43 cases of profound hearing loss. DPOAE was absent in the affected ear in all subjects, except for two patients with unilateral profound hearing loss with CNC stenosis and narrow IAC without cochlear/vestibular/semicircular canal malformations. These two patients demonstrated normal responses in DPOAE in both ears. In one of these cases, ABR was performed. The threshold of wave V was 95 dBnHL (normal Hearing Level) in the affected ear and 20 dBnHL in the normal ear. This case was confirmed as unilateral auditory

Table 3
Relationship between cochlear nerve canal malformations and internal auditory canal malformations.

Cochlear nerve canal		Internal auditory canal	
Stenosis	32 (46.4%)	Narrow	16 (50.0%)
		Normal	16 (50.0%)
Normal	36 (52.2%)	Narrow	4 (11.1%)
		Normal	31 (86.1%)
		Large	1 (2.8%)
Absent	1 (1.4%)	Absent	1 (100.0%)

Table 4
Combination of malformations and hearing level.

Cochlear nerve canal stenosis		+				–				Total
Narrow internal auditory canal		+		–		+		–		
Cochlear/vestibular/semicircular canal malformations		+	–	+	–	+	–	+	–	
Hearing level	Mild (21–40 dB)			1			1		4	6
	Moderate (41–70 dB)	1			3		1	4	4	13
	Severe (71–95 dB)	2			1			1	3	7
	Profound (>95 dB)	4[a]	10[b]	2	9		2	4	12	43
Total		7	10	3	13		4	9	23	69

[a] One patient had common cavity with IAC deficiency.
[b] Two patients demonstrated normal distortion product otoacoustic emissions.

neuropathy spectrum disorder. There were no correlations between the hearing level and the existence of CNC stenosis, narrow IAC, or other malformations in subjects with absence of DPOAE.

4. Discussion

The data in the present study showed a high prevalence of inner-ear and/or IAC malformations in pediatric USNHL. The prevalence was 84.6% in infants younger than 1 year of age. Most USNHL in these infants was considered as congenital, implying that more than 80% of the congenital USNHL was caused by morphological abnormality accompanied with bony anomalies.

The frequency of reported abnormal temporal bone findings in patients with USNHL varies from 7% to 44% [7]. Song et al. [8] studied CT of 322 children with USNHL and reported that 28.9% had malformations. Simons et al. [7] reported that the prevalence of CT abnormalities was 35% (29 of 83 cases), and the prevalence of magnetic resonance imaging (MRI) abnormalities was 25% (10 of 40 cases) in children with USNHL. However, they did not refer to the CNC.

The size of the CNC was first reported by Fatterpekar et al. in 2000 [5]. They demonstrated that the length and width of the CNC were significantly smaller ($p < 0.05$) in patients with congenital SNHL who had "normal" findings at thin-section temporal bone CT than in the control group. In 2008, Kono [3] investigated 118 patients without inner-ear malformations among 160 patients with USNHL, and 60% showed a significant difference in the CNC diameters between the affected and unaffected sides. Kono suggested that a diameter of less than 1.7 mm on transverse images or less than 1.8 mm on coronal images was hypoplasia. Stjernholm et al. [12] suggested that if the CNC diameter was less than 1.4 mm, then the possibility of cochlear nerve abnormality should be considered. Recent studies [9,13] demonstrated that CNC stenosis with a diameter of 1.5 mm or less as assessed with CT suggested cochlear nerve deficiency or hypoplasia as assessed with MRI. Wilkins et al. [14] showed a significant correlation between the degree of CNC stenosis and the degree of hearing loss. In the present study with the definition that the diameter was less than 1.5 mm, 46.4% of the subjects had CNC stenosis.

The exact cause of narrow CNC is unclear. Proper development of the IAC requires the presence of a normal cochlear nerve as a stimulus for attaining normal adult dimensions [5]. There is a possibility that the normal development of the CNC similarly needs the nerve for stimulus [5,15]. Fatterpekar et al. [5] speculated that, in patients with abnormality involving the membranous labyrinth, inhibition of the normal trophic effects of nerve growth factors owing to a diminutive cochlear nerve results in a small CNC. That is to say, hypoplasia of the CNC might be secondary to a hypoplastic cochlear nerve associated with some abnormality of a membranous labyrinth that could not be detected by current imaging techniques [3]. Very few of our subjects demonstrated a positive response in DPOAE, suggesting that at least the outer hair cells were affected or may not exist in most patients with USNHL.

The abnormalities found by imaging techniques provide information for diagnosis, management of hearing loss, and genetic and lifestyle counseling [1,6]. Congenital malformed inner ears may be associated with cerebrospinal fluid leakage, and thus development of meningitis is a very real possibility. Parents of children with inner-ear anomalies should be informed of the early symptoms and signs of meningitis. Consideration also should be given to immunization against common organisms implicated in meningitis [16]. Genetic examination should be recommended for patients with enlarged vestibular aqueducts. Pourova et al. [17] recommend performing SLC26A4 mutation analysis, following GJB2 analysis, in all hearing loss patients with bilateral enlarged vestibular aqueduct and/or associated thyroid impairment. Thy also mentioned that it is not reasonable to test the SLC26A4 gene in children with sporadic deafness without knowledge of their temporal bone CT/MRI images or even with its normal result. Mutations in the SLC26A4 are responsible for Pendred syndrome [18] as well as DFNB4 (non-syndromic hearing loss with inner ear abnormalities—enlarged vestibular aqueduct and/or Mondini deformity) [19]. Pendred syndrome and bilateral enlarged vestibular aqueduct correlates with the presence of two mutant alleles of *SLC26A4* [17,20,21]. Hearing loss in most patients with *SLC26A4* mutations fluctuates and is progressive [22]. Mutations in *SLC26A4* indicate the necessity for careful management of hearing and comorbidities, such as goiter.

The lack of MRI examination is one of the limitations in the present study. The results suggest the importance of temporal bone CT. Nevertheless, the risks of sedation/anesthesia for imaging in infants and young children, or indeed the radiation risk should be considered. The ideal imaging algorithm in children with unilateral or asymmetric SNHL is controversial [7]. MRI can detect soft-tissue abnormalities such as cochlear nerve deficiency with normal CNC and IAC. Simons et al. [7] suggested that virtually all children with SNHL should have an imaging study as part of their workup. They prefer high-resolution temporal bone CT as the initial study because of a high prevalence of positive findings and less cumbersome logistical issues. They also recommended that a negative CT scan should be followed by MRI to rule out SNHL caused by the central nervous system.

There are some other limitations regarding the current study. The first limitation is the diagnosis of SNHL. USNHL was determined on the basis of ABR and ASSR in 34 young patients. Middle-ear diseases and abnormalities were ruled out by CT and tympanometry; however, there is a possibility that some patients had conductive or combined hearing loss. Another limitation concerns the number of subjects. We examined 69 children, however, the evaluations should be need in the larger group.

In conclusion, a high prevalence of inner-ear and/or IAC malformations was detected by high-resolution temporal bone CT in children with USNHL. Radiological and genetic examination provided important information concerning the pathogenesis and management of hearing loss. The results of this study supported the recommendation of temporal bone CT to children with USNHL early in life. Genetic examination of *SLC26A4* also should be performed in all cases with bilateral enlarged vestibular aqueduct. The study in the larger group will likely refine the clinical protocol.

Acknowledgment

This research was supported by a Grant-in-Aid for Clinical Research from the National Hospital Organization, Tokyo, Japan.

References

[1] J.E. McClay, R. Tandy, K. Grundfast, S. Choi, G. Vezina, G. Zalzal, et al., Major and minor temporal bone abnormalities in children with and without congenital sensorineural hearing loss, Arch. Otolaryngol. Head Neck Surg. 128 (2002) 664–671.
[2] J.D. Swartz, H.R. Harnsberger, The otic capsule and otodystrophies, in: J.D. Swartz, H.R. Harnsberger (Eds.), Imaging of the Temporal Bone, 3rd ed., Thieme, New York, 1998, pp. P240–P266.
[3] T. Kono, Computed tomographic features of the bony canal of the cochlear nerve in pediatric patients with unilateral sensorineural hearing loss, Radiat. Med. 26 (2008) 115–119.
[4] L. Sennaroglu, I. Saatci, A new classification for cochleovestibular malformations, Laryngoscope 112 (2002) 2230–2241.
[5] G.M. Fatterpekar, S.K. Mukherji, J. Alley, Y. Lin, M. Castillo, Hypoplasia of the bony canal for the cochlear nerve in patients with congenital sensorineural hearing loss: initial observations, Radiology 215 (2000) 243–246.
[6] R.S. Yiin, P.H. Tang, T.Y. Tan, Review of congenital inner ear abnormalities on CT temporal bone, Br. J. Radiol. 84 (2011) 859–863.
[7] J.P. Simons, D.L. Mandell, E.M. Arjmand, Computed tomography and magnetic resonance imaging in pediatric unilateral and asymmetric sensorineural hearing loss, Arch. Otolaryngol. Head Neck Surg. 132 (2006) 186–192.
[8] J.J. Song, H.G. Choi, S.H. Oh, S.O. Chang, C.S. Kim, J.H. Lee, Unilateral sensorineural hearing loss in children: the importance of temporal bone computed tomography audiometric follow-up, Otol. Neurotol. 30 (2009) 604–608.
[9] M. Miyasaka, S. Nosaka, N. Morimoto, H. Taiji, H. Masaki, CT and MR imaging for pediatric cochlear implantation: emphasis on the relationship between the cochlear nerve canal and the cochlear nerve, Pediatr. Radiol. 40 (2010) 1509–1516.
[10] B. Coyle, W. Reardon, J.A. Herbrick, L.C. Tsui, E. Gausden, J. Lee, et al., Molecular analysis of the Pds gene in Pendred syndrome (sensorineural hearing loss and goitre), Hum. Mol. Genet. 7 (1998) 1105–1112.
[11] Y.Y. Yuan, P. Dai, Q.W. Zhu, D.Y. Kang, D.L. Huang, Sequencing analysis of whole SLC26A4 gene related to IVS7-2A>G mutation in 1552 moderate to profound sensorineural hearing loss patients in China, Zhonghua Er Bi Yan Hou Tou Jing Wai Ke Za Zhi 44 (2009) 449–454.
[12] C. Stjernholm, C. Muren, Dimensions of the cochlear nerve canal: a radioanatomic investigation, Acta Otolaryngol. 122 (2002) 43–48.
[13] S. Komatsubara, A. Haruta, Y. Nagano, T. Kodama, Evaluation of cochlear nerve imaging in severe congenital sensorineural hearing loss, ORL J. Otorhinolaryngol. Relat. Spec. 69 (2007) 198–202.
[14] A. Wilkins, S.P. Prabhu, L. Huang, P.B. Ogando, M.A. Kenna, Frequent association of cochlear nerve canal stenosis with pediatric sensorineural hearing loss, Arch. Otolaryngol. Head Neck Surg. 138 (2012) 383–388.
[15] J.W. Casselman, F.E. Offeciers, P.J. Govaerts, R. Kuhweide, H. Geldof, T. Somers, et al., Aplasia and hypoplasia of the vestibulocochlear nerve: diagnosis with MR imaging, Radiology 202 (1997) 773–781.
[16] P.G. Reilly, A.K. Lalwani, R.K. Jackler, Congenital anomalies of the inner ear, in: Pediatric Otology and Neurotology, Lippincott-Raven Publishers, Philadelphia, 1998, pp. 201–210.
[17] R. Pourová, P. Janousek, M. Jurovcík, M. Dvoráková, M. Malíková, D. Rasková, et al., Spectrum and frequency of SLC26A4 mutations among Czech patients with early hearing loss with and without Enlarged Vestibular Aqueduct (EVA), Ann. Hum. Genet. 74 (2010) 299–307.
[18] L.A. Everett, B. Glaser, J.C. Beck, J.R. Idol, A. Buchs, M. Heyman, et al., Pendred syndrome is caused by mutations in a putative sulphate transporter gene (PDS), Nat. Genet. 17 (1997) 411–422.
[19] S.P. Pryor, A.C. Madeo, J.C. Reynolds, N.J. Sarlis, K.S. Arnos, W.E. Nance, et al., SLC26A4/PDS genotype-phenotype correlation in hearing loss with enlargement of the vestibular aqueduct (EVA): evidence that Pendred syndrome and non-syndromic EVA are distinct clinical and genetic entities, J. Med. Genet. 42 (2005) 159–165.
[20] C.C. Wu, Y.C. Lu, P.J. Chen, P.L. Yeh, Y.N. Su, W.L. Hwu, et al., Phenotypic analyses and mutation screening of the SLC26A4 and FOXI1 genes in 101 Taiwanese families with bilateral nonsyndromic enlarged vestibular aqueduct (DFNB4) or Pendred syndrome, Audiol. Neurootol. 15 (2010) 57–66.
[21] T. Ito, B.Y. Choi, K.A. King, C.K. Zalewski, J. Muskett, P. Chattaraj, et al., SLC26A4 genotypes and phenotypes associated with enlargement of the vestibular aqueduct, Cell. Physiol. Biochem. 28 (2011) 545–552.
[22] H. Suzuki, A. Oshima, K. Tsukamoto, S. Abe, K. Kumakawa, K. Nagai, et al., Clinical characteristics and genotype–phenotype correlation of hearing loss patients with SLC26A4 mutations, Acta Otolaryngol. 127 (2007) 1292–1297.

Functional Interaction Between Mesenchymal Stem Cells and Spiral Ligament Fibrocytes

Guang-wei Sun,[1]* Masato Fujii,[2] and Tatsuo Matsunaga[1]*

[1]The Laboratory of Auditory Disorders, National Institute of Sensory Organs, National Tokyo Medical Center, Tokyo, Japan
[2]Division of Hearing and Balance Research, National Institute of Sensory Organs, National Tokyo Medical Center, Tokyo, Japan

Spiral ligament fibrocytes (SLFs) play an important role in normal hearing as well as in several types of sensorineural hearing loss attributable to inner ear homeostasis disorders. Our previous study showed that transplantation of mesenchymal stem cells (MSCs) into the inner ear of rats with damaged SLFs significantly accelerates hearing recovery compared with rats without MSC transplantation. To elucidate this mechanism of SLF repair and to determine the contribution of transplanted MSCs in this model, we investigated the mutual effects on differentiation and proliferation between MSCs and SLFs in a coculture system. Factors secreted by SLFs had the ability to promote the transdifferentiation of MSCs into SLF-like cells, and the factors secreted by MSCs had a stimulatory effect on the proliferation of SLFs. Cytokine antibody array analysis revealed the involvement of transforming growth factor-β (TGF-β) in SLF proliferation induced by MSCs. In addition, a TGF-β inhibitor reduced SLF proliferation induced by MSC stimulation. Our results suggest that there are two mechanisms of hearing recovery following transplantation of MSCs into the inner ear: 1) MSCs transdifferentiate into SLF-like cells that compensate for lost SLFs, and 2) transplanted MSCs stimulate the regeneration of host SLFs. Both mechanisms contribute to the functional recovery of the damaged SLF network.

Key words: mesenchymal stem cells; spiral ligament fibrocytes; transplantation

Mammalian cochlear fibrocytes of the mesenchymal nonsensory regions play an important role in the cochlear physiology of hearing, including the transport of potassium ions to generate an endocochlear potential in the endolymph that is essential for the transduction of sound by hair cells (Weber et al., 2001; Wangemann, 2002; Delprat et al., 2005). Recent studies have also highlighted the importance of these fibrocytes in the spiral ligament (SL) in the pathogenesis of sensorineural hearing loss. Several studies have indicated the involvement of SL degeneration in the mechanism of hearing loss that is due to aging (Hequembourg and Liberman, 2001; Spicer and Schulte, 2002), excessive noise (Hirose and Liberman, 2003), or genetic mutations (Minowa et al., 1999).

The spiral ligament fibrocytes (SLFs) are divided into types I–V based on their structural features, immunostaining patterns, and general location (Spicer and Schulte, 1996). In contrast to sensory cells, SLFs are able to repopulate themselves after noise or drug exposure in the mammalian inner ear (Roberson and Rubel, 1994; Hirose and Liberman, 2003; Lang et al., 2003). We previously developed a rat model of acute sensorineural hearing loss attributable to the dysfunction of SLFs induced by a mitochondrial toxin, 3-nitropropionic acid (3NP; Hoya et al., 2004; Okamoto et al., 2005; Kamiya et al., 2007; Mizutari et al., 2011). The main cause of hearing loss in this model is apoptosis of SLFs, without any changes in the organ of Corti. In addition, hearing recovery that occurs after 3NP exposure is accompanied by the regeneration of SLFs (Kamiya et al., 2007; Mizutari et al., 2011). The reconstruction of the potassium recycling route by SLF regeneration might lead to normalization of the endocochlear potential and hearing recovery.

After mesenchymal stem cells (MSCs) are transplanted into the inner ear of 3NP-treated rats, some of these stem cells are detected in the injured area of the SL, which correlates with a significantly greater hearing

Contract grant sponsor: Ministry of Education, Culture, Sports, Science and Technology of Japan; Contract grant number: 20591996 (to G.-w.S.); Contract grant sponsor: Ministry of Health, Labour, and Welfare of Japan; Contract grant number: H16-Kankakuki-006 (to T.M.).

*Correspondence to: Guang-wei Sun, The Laboratory of Biomedical Material Engineering, Dalian Institute of Chemical Physics, The Chinese Academy of Sciences, 457 Zhongshan Rd., Dalian 116023, China. E-mail: sunrise124@gmail.com. or Tatsuo Matsunaga, The Laboratory Auditory Disorders, National Institute of Sensory Organs, National Tokyo Medical Center, 2-5-1 Higashigaoka, Meguro, Tokyo 152-8902, Japan. E-mail: matsunagatatsuo@kankakuki.go.jp

Received 29 August 2011; Revised 3 March 2012; Accepted 20 March 2012

Published online in Wiley Online Library (wileyonlinelibrary.com). DOI: 10.1002/jnr.23067

recovery than occurs in control animals. The transplanted MSCs in the SL also express gap junction proteins between neighboring cells (Kamiya et al., 2007). The number of transplanted MSCs detected in the SL did, however, lead us to question whether those MSCs are sufficient for the supplementation of lost SLFs. To elucidate the mechanism of hearing recovery by MSC transplantation, we investigated the interaction between MSCs and SLFs as well as possible signaling mechanisms that may be involved in this interaction.

MATERIALS AND METHODS

Composition of Media and Growth Factors

Minimum essential medium (MEM) and RPMI 1640 supplemented with 9% fetal calf serum (FCS) were obtained from Invitrogen (Carlsbad, CA). Recombinant human transforming growth factor-β1 (TGF-β1) and TGF-β3 (R&D Systems, Minneapolis, MN) were used at a final concentration of 10 ng/ml. SB-431542 (Sigma-Aldrich, St. Louis, MO) and SU4984 (Calbiochem, Ober der Roth, Germany) were each added to cells at a concentration of 10 μM.

Antibodies

The antibodies used in this study are as follows: Na^+/K^+-ATPase α-1 and Na^+/K^+-ATPase β-1 (Santa Cruz Biotechnology, Santa Cruz, CA); Na-K-2Cl cotransporter (NKCC1; ARP, Belmont, MA); connexin 31 (Cx31; Zymed, Carlsbad, CA); vimentin and aquaporin 1 (Abcam, Cambridge, MA); S-100 (Sigma-Aldrich); CD16/32, CD45, CD44, mouse IgG2a isotype control, and mouse IgG2b isotype control (eBioscience, San Diego, CA); and CD29, CD49e, and streptavidin-fluorescein isothiocyanate (BD Pharmingen, San Diego, CA). The appropriate species-specific antibodies conjugated to either Alexa Fluor 488 or Alexa Fluor 568 (1:500; Molecular Probes, Eugene, OR) were used as secondary antibodies.

Cell Culture

Male C3H/HeJJcl mice (6 weeks old and postnatal day [P] 0) were used in the present study. All experiments were conducted in accordance with the guidelines of the National Institutes of Health and the Declaration of Helsinki. After anesthetization with xylazine (15 mg/kg, i.p.) and ketamine (80 mg/kg, i.p.), the mice were sacrificed. The inner ears were harvested rapidly, and the SLs from two ears were dissected at 4°C under aseptic conditions. The stria vascularis was carefully removed from the SLs using tweezers. The entire SL segment was collected and minced into small pieces with corneal scissors. The minced pieces were placed in type I collagen-coated Petri dishes (BD Pharmingen) in MEM supplemented with 9% FCS. The dish was kept in an incubator (37°C; 5% CO_2, 95% air) with maximum humidity, and the culture medium was changed every 3 days. Cells from passages 2–4 were stored with Cell Banker reagent (Juji Field, Tokyo, Japan) at −80°C.

We prepared MSCs as described by Islam et al. (2006). Briefly, to initiate the MSC cultures, bone marrow cells from C3H/HeJJcl mice were plated in tissue culture dishes and kept in a humidified incubator with 5% CO_2 at 37°C for 72 hr, at which point nonadherent cells were removed by changing the medium. The primary culture was then trypsinized and passaged to a new culture dish with a split ratio of 1:2. Subsequent passages were done when the culture approached confluence. Cells from passages 5–10 were used for the present investigation.

Culture medium from MSCs or SLFs was filtered with a 0.22-μm syringe filter (Millipore, Billerica, MA) to remove cells and was then used as conditioned medium. The conditioned medium was added to cells at a 1:1 (vol/vol) ratio with standard medium. For effects on cell cultures, MSCs and SLFs were plated on Petri dishes with standard medium for 3 days and then cultured with conditioned medium.

Flow Cytometry

Cells were incubated with antibodies for 30 min on ice and then centrifuged at 200*g* for 5 min. The antibody solution was removed, and cells were resuspended in ice-cold Hank's medium (Invitrogen) containing 2 μg/ml propidium iodide (Sigma-Aldrich) to distinguish between dead and living cells. The surface markers expressed on these cells were then analyzed by flow cytometry (Epics Altra with HyPerSort cell sorting system; Beckman Coulter, Fullerton, CA).

Immunocytochemical Staining

SLFs and MSCs placed on the Lab-Tek Chamber Slide System (Nunc, Rochester, NY) or in BD Falcon Cell Culture flasks (BD Pharmingen) were cultured with or without conditioned medium. Cultured cells were fixed in 4% paraformaldehyde (PFA). For the cells cultured in flasks, fixed cells were attached to slides with the cytospin method. Incubation with primary and secondary antibodies was carried out in phosphate-buffered saline (PBS) containing 1% normal goat serum (Sigma-Aldrich) overnight at 4°C or for 1 hr at room temperature. For negative controls, the primary antibody was omitted. Nuclear staining was performed with 4′6-diamidino-2-phenylindole dihydrochloride (DAPI; Sigma-Aldrich). The specimens were viewed with a laboratory microscope (DM 2500; Leica, Houston, TX).

Immunocytochemistry of Tissue Sections

Inner ears were isolated from male C3H/HeJJcl mice. Paraffin-embedded temporal bone blocks were sectioned horizontally at 5 μm. After deparaffinization, the sections were blocked with 10% normal goat serum (Sigma-Aldrich) diluted in 0.01 M PBS for 1 hr at room temperature. Incubation with primary and secondary antibodies was carried out in PBS containing 1% normal goat serum overnight at 4°C or for 1 hr at room temperature. For negative controls, the primary antibody was omitted. Nuclear staining was performed with DAPI. The appropriate species-specific antibodies conjugated to either Alexa Fluor 488 or Alexa Fluor 568 were used as secondary antibodies. The specimens were viewed with the DM 2500 microscope (Leica, Houston, TX).

DNA Arrays

The following cells were compared: 1) untreated MSCs (control) and MSCs cultured for 1 week with conditioned

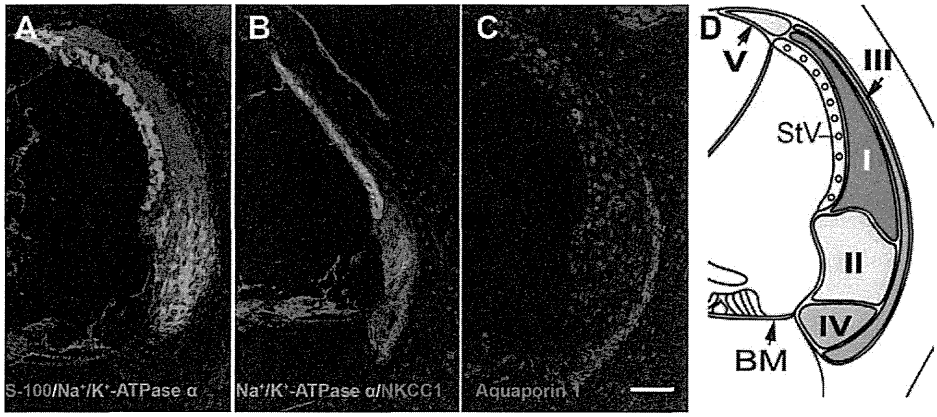

Fig. 1. Lateral wall from the middle turn of a C3H/HeJJcl mouse cochlea. **A–C:** Sections stained for S-100 (A), Na^+/K^+-ATPase α1 (A,B), NKCC1 (B), and aquaporin 1 (C) are shown. Type I fibrocytes of the SL were positive for S-100. Type II and type V fibrocytes also stained with antibodies to S-100, Na^+/K^+-ATPase α1, and NKCC1; however, they were distinguishable from type IV fibrocytes by their positive staining for S-100 and Na^+/K^+-ATPase α1. Type III fibrocytes were positive for aquaporin 1 (C). **D:** Illustration of the lateral wall region shown in A–C, with the fibrocyte populations indicated. BM, basilar membrane; StV, stria vascularis. Scale bar = 50 μm.

medium from SLFs and 2) untreated SLFs (control) and SLFs cultured for 1 week with conditioned medium from MSCs (n = 1). Isolation of RNA, hybridization, and cDNA array analyses were performed by Filgen (Agilent Technologies Inc., Tokyo, Japan) using OpArray mouse v4.0 (Filgen). The Microarray Data Analysis Tool, version 1.5 (Filgen), was used to quantify signal intensities. As per the manufacturer's instructions (Filgen), changes in mRNA expression were considered meaningful if there was a greater than twofold change relative to the control values. Data were analyzed using Microarray Data Analysis Tool, version 3.2 (Filgen).

Cytokine Antibody Arrays

When MSCs were nearly confluent, they were cultured in RPMI 1640 with 0.2% FCS for 24 hr. The medium was harvested and filtered with a 0.22-μm syringe filter to remove cell debris (n = 1). Cytokine antibody array analyses were performed by Filgen using a RayBio biotin label-based mouse cytokine antibody array (L-308; RayBiotech, Norcross, GA). The quantified secretion of each cytokine was compared as a ratio using Microarray Data Analysis Tool, version 1.5. Changes in cytokine secretion were considered meaningful if there was a greater than twofold change relative to the control values.

Statistical Analysis

All statistical analyses were performed using a one-way analysis of variance. OriginPro 7.5 (OriginLab, Northampton, MA) was used for comparisons between experimental groups and control groups. $P < 0.01$ was considered significant.

RESULTS

Histological Observations

The staining pattern of cells that make up the cochlea from a 6-week-old C3H/HeJJcl mouse is shown in Figure 1. Type I SLFs, which are found lateral to the stria vascularis (Takahashi and Kimura, 1970), showed positive immunological staining for S-100 (Fig. 1A). These fibrocytes did not show staining for Na^+/K^+-ATPase α1 (Fig. 1A,B) or NKCC1 (Fig. 1B). Type II fibrocytes, which are located lateral to the spiral prominence (Takahashi and Kimura, 1970), and type V fibrocytes, which are equivalent to the type II fibrocytes in the suprastrial region (Spicer and Schulte, 1996), were positive for Na^+/K^+-ATPase α1 (Fig. 1A,B) and NKCC1 (Fig. 1B) staining. Type II and type V fibrocytes were also positive for S-100 staining (Fig. 1A). Aquaporin 1 staining was detected on type III fibrocytes only (Fig. 1C), which are found adjacent to the bone in the inferior region of the SL (Spicer and Schulte, 1991). Type IV fibrocytes, which are located inferior to the basilar membrane (Spicer and Schulte, 1991), were distinguishable from type II fibrocytes because they were positive for NKCC1 and negative for Na^+/K^+-ATPase α1 and S-100 staining in these mice (Fig. 1A,B). The immunohistochemical profile of SLFs is shown in Table I. Each type of SLF could be distinguished based on its pattern of antibody staining.

TABLE I. Immunohistochemical Profile of SLF Types in C3H/HeJJcl Mice

Antigen	Type I	Type II/V	Type III	Type IV
S-100	+	+	−	−
Na^+/K^+-ATPase α1	−	+	−	−
NKCC1	−	+	−	+
Aquaporin 1	−	−	+	−

Observations of the Growth and Differentiation of Cultured SLFs

The first signs of growth in the SL explants were observed within 24–48 hr. Cell expansion was observed

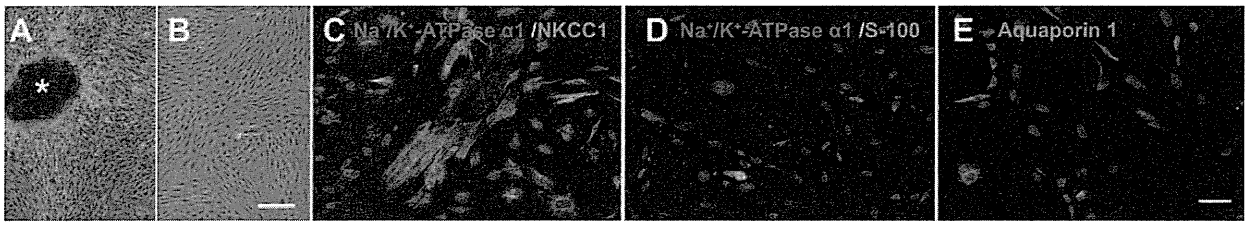

Fig. 2. Pure cultures of postnatal mice SLFs were obtained and stably maintained in vitro. **A:** Primary culture of SLFs after 21 days in culture. Spindle-shaped cells extending from the edges of the explant (asterisk) were observed. **B:** Cells that had been passaged one time with homogenous morphology. The expression of each type-specific set of SLF markers was detected in cultured SLFs. **C–E:** Na^+/K^+-ATPase α1 (type II), NKCC1 (type II and IV), S-100 (type I and II), aquaporin 1 (type III). Scale bars = 50 μm in A (applies to A,B); 50 μm in E (applies to C–E).

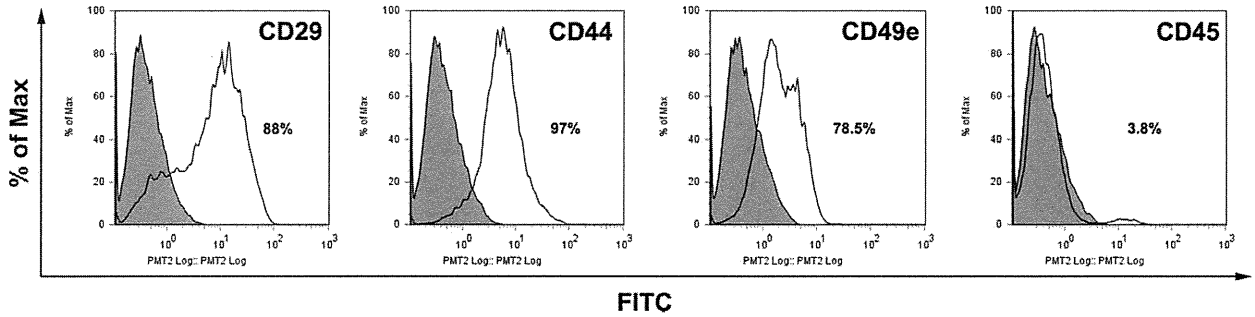

Fig. 3. Characterization of MSCs. MSCs at passages 5 and 10 were positive for CD29, CD44, and CD49e staining and were negative for CD45 staining. Open areas show the percentages of positive cells; shaded areas show cells treated with isotope antibodies.

initially as spindle-shaped cells extending from the edges of the explants (Fig. 2A). The primary culture was subcultured at 21 days. Spindle-shaped cells having large nuclei and cytoplasmic regions with slender, irregular processes were observed (Fig. 2B). The morphological characteristics of the subculture were consistent with previous studies (Gratton et al., 1996; Suko et al., 2000). The number of SLFs significantly increased in the adherent culture (by ~ 376-fold after 21 days in culture; see Fig. 4F). Type I SLFs were positive for S-100 staining but negative for Na^+/K^+-ATPase α1 and NKCC1 staining. Type II SLFs were positive for Na^+/K^+-ATPase α1, NKCC1, and S-100 staining. Type III SLFs were positive for aquaporin 1 staining only, whereas type IV SLFs were positive for NKCC1 staining (Fig. 2C–E, Table I). These results suggested that this culture system included all types of SLFs. Most of the cells in this culture system were type II (34.06%) and type IV (62.64%) fibrocytes. The percentages of type I and type III fibrocytes were 2.2% and 13.2%, respectively.

Characterization of MSCs

MSC cells from passages 5 and 10 were used for investigation of cell surface markers. Flow cytometry analysis indicated that these MSCs were positive for CD29, CD44, and CD49e staining but were negative for CD45 staining (Fig. 3) before transplantation, which is similar to previously isolated murine MSCs (Islam et al., 2006).

Effects of MSC Culture Supernatants on SLFs

Next, the effect of molecules secreted by MSCs on SLFs was investigated. The addition of culture supernatants from MSCs markedly stimulated the proliferation of SLFs (twofold) after 21 days in vitro (Fig. 4F). To ascertain whether the cellular characteristics were affected by the molecules secreted by MSCs, we checked the expression of SLF markers on those cells. Previous studies have indicated that the fibrocyte populations that are most likely to show degeneration in the damaged cochlea are the type II and IV fibrocytes (Kamiya et al., 2007). Thus we focused here on investigating the expression of type II and IV markers. Immunostaining showed that the expression of SLF type markers decreased, whereas the percentage of vimentin-positive cells increased, in SLFs cultured with MSC conditioned medium compared with the expression in SLFs cultured without the conditioned medium (Fig. 4A,B,E). Vimentin is a marker of mesenchymal cells and is detected in the mesenchyme-derived tissue of the inner ear (Kuijpers et al., 1992). Increases in vimentin synthesis are associated with rapidly growing cells (Benzeev, 1985). In our study, vimentin immunoreactivity was observed in almost all SLFs in P0 C3H/HeJJcl mice (Fig. 4C), whereas no NKCC1 was detected (data

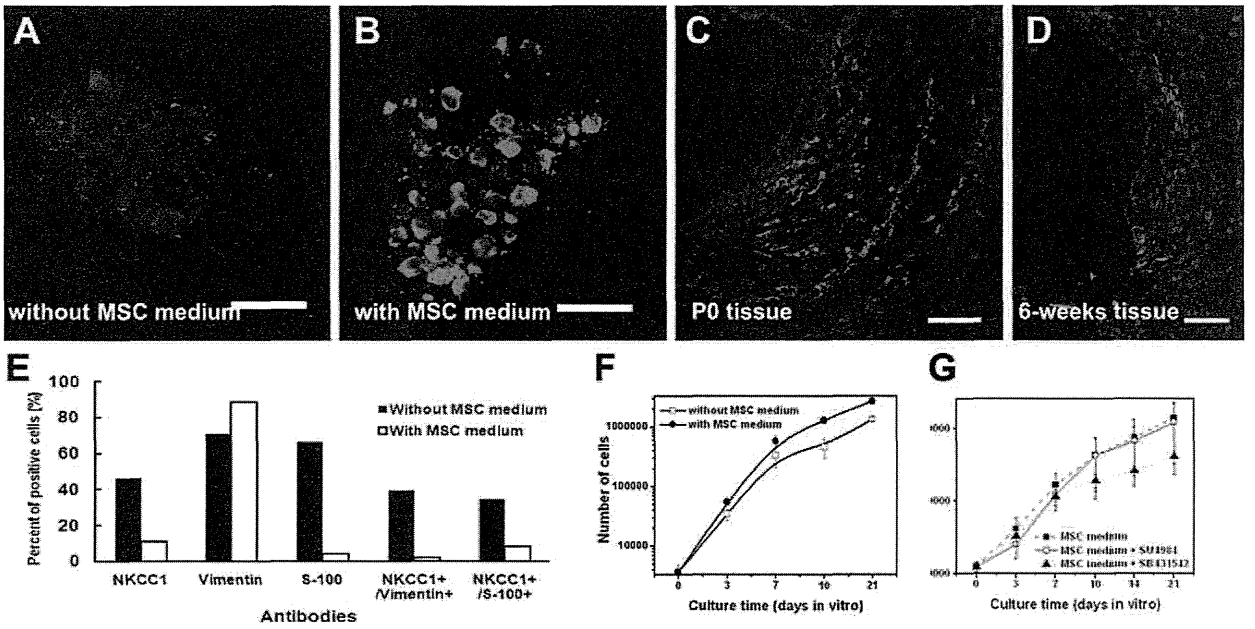

Fig. 4. Characteristics of SLFs cultured with or without culture supernatants from MSCs for 21 days. Vimentin expression increased in SLFs in culture in the presence of MSC conditioned medium (**B**) but not in its absence (**A**). **C:** In P0 C3H/HeJJcl mice, strong vimentin immunoreactivity was observed in fibrocytes of the SL. **D:** At 6 weeks after birth, vimentin expression was restricted to a subgroup of the SLFs. **E:** Expression of vimentin in SLFs in the absence or presence of MSC conditioned medium. **F:** Growth curves of SLF cells cultured with or without MSC conditioned medium. **G:** SLF proliferation stimulated by MSC conditioned medium was inhibited by the addition of SB-431542 and SU4984. The percentage of the cells in each bar chart indicates the mean ± SD of three independent experiments. Nuclei were stained with DAPI (blue). Scale bars = 50 μm.

not shown). At 6 weeks after birth, vimentin expression was restricted to a subpopulation of SLFs (Fig. 4D). Our results suggest that factors in the supernatants of MSCs grown in culture have the ability to stimulate the proliferation of SLFs and that a high proportion of these proliferating SLFs has marker expression features that are similar to those of SLFs early in postnatal development.

Effects of SLF Culture Supernatants on MSCs

To investigate whether SLF conditioned medium has effects on the proliferation and differentiation of MSCs, MSCs were cultured with or without conditioned medium. In the initial cultures, no MSCs were positive for Na^+/K^+-ATPase β1 (Fig. 5A) or NKCC1 (data not shown) expression, both of which are type II and IV SLF marker proteins (Schulte and Steel, 1994). After the culture, although MSC-derived cells expressed Na^+/K^+-ATPase β1 spontaneously, the addition of SLF conditioned medium increased the expression of Na^+/K^+-ATPase β1 (Fig. 5B) compared with MSC cultures without the conditioned medium (Fig. 5E; $P < 0.05$). Some MSC-derived cells were also positive for NKCC1 expression (Fig. 5C). No cells that were positive for S-100 expression were detected in the initial MSC cultures (data not shown). With culture on collagen-coated dishes at a low density, S-100-positive cells were, however, detected (data not shown). The proportion of S-100-positive cells was not affected by the addition of SLF conditioned medium (Fig. 5D; 62.4% vs. 69.72%, 14 days in vitro).

We also examined the effects of conditioned medium from SLFs on MSC proliferation. The total number of cells obtained after the addition of SLF conditioned medium was similar to that obtained with standard medium (Fig. 5F; $P = 0.718$). Our results suggest that the factors secreted by SLFs promote MSC transdifferentiation into SLF-like cells but do not affect MSC proliferation.

Cell Microarray Analysis and Cell Proliferation Assay

To investigate the underlying cellular and molecular differences between the cells cultured in standard medium and those cultured with conditioned medium, we performed a gene expression analysis on both MSCs and SLFs using the OpArray mouse v4.0 array. Significant changes in gene expression were filtered according to the background expression of individual genes and at least a twofold difference in expression between the samples and controls. Detailed examination of the biological functions of differentially expressed genes between MSCs with or without SLF conditioned medium revealed genes related to stem cell development, the

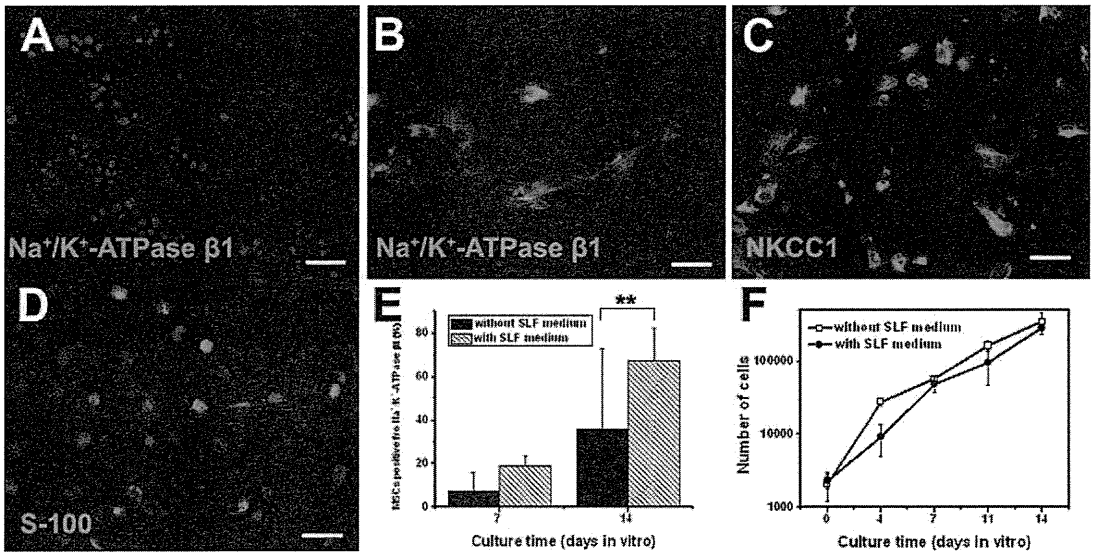

Fig. 5. Characteristics of MSCs cultured with or without culture supernatants from SLFs. **A:** SLF-like cell differentiation of MSCs. No cells that were positive for Na^+/K^+-ATPase β1 expression were found in the initial MSC cultures. **B,E:** When MSCs were plated on collagen-coated dishes, the addition of SLF conditioned medium (with SLF) increased the expression of Na^+/K^+-ATPase β1 (B,E) compared with cultures without conditioned medium (E; $^{**}P < 0.05$). **C,D:** Furthermore, cells that were positive for the expression of NKCC1 (C) and S-100 (D) were detected in MSCs cultured with SLF conditioned medium. **F:** Conversely, culture supernatants from SLFs had no effect on promoting the proliferations of MSCs. The percentage of the cells in each bar chart indicates the mean ± SD of three independent experiments. Nuclei were stained with DAPI (blue). Scale bars = 50 μm.

TABLE II. Genes Differentially Expressed Between MSCs Cultured With and Without SLF Conditioned Medium

Category	Increased by more than twofold	Decreased by more than twofold
Stem cell development	*Tfrc, Tnfrsf12a, Ednrb, Ncam, Hells, Grem1, Slc2a1, Ccna2, S100a4, Angpt1, Mmp14*	*Wif1, Ascl1, Ibsp, Myod1, Col4a6, Thbs1, Prok2, Mmp13, phex, Mtss1*
Wnt pathway	*Pitx2, Wnt8a*	*Wif1*
Cell cycle	*Nek2, Ccna2, Mcm3*	*Trp63*
Apoptosis	*Hmox1, Tnfrsf12a, Hells, Lhx4*	*Myod1, Trp63, Gadd45b, Thbs1, Prok2, Dffb*

TABLE III. Genes Differentially Expressed Between SLFs Cultured With and Without MSC Conditioned Medium

Category	Increased by more than twofold	Decreased by more than twofold
Extracellular matrix and adhesion molecules	*Spp1, Tgfbi*	*Mmp11, Thbs1*
Wnt pathway		*Wisp2*
Notch pathway	*Dtx3, Gli2*	
TGF-β, BMP pathway	*Tgfbi*	
Apoptosis	*Pttg1, Lhx4, Atf5, Cyp2c38*	*Thbs1*
Growth factors	*Spp1*	
Cytokine and inflammatory responses	*Spp1, Atf5, tgfbi, Ifit1*	

Wnt pathway, the cell cycle, and apoptosis (Table II). In contrast, between SLFs cultured with or without MSC conditioned medium, genes involved in extracellular matrix and adhesion molecules, apoptosis, and cytokine and inflammatory responses as well as key determinants of cell fate (Wnt pathway, Notch pathway, and TGF-β pathway) were significantly different (Table III).

Furthermore, by using an array that focuses on mouse cytokines, we investigated factors secreted by MSCs. Ten factors were increased more than twofold in MSC conditioned medium compared with the medium in which no cells were cultured. The biological functions of those cytokines are related to apoptosis, the inflammatory response, and cell proliferation (data not shown). One of the secreted cytokines was TGF-β3, which is involved in cell proliferation (Huang and Huang, 2005). To determine the TGF-β responsible for regulating SLF proliferation, SB-431542, a specific inhibitor of the TGF-β type I receptor (TbRI; Laping et al., 2002), was added to MSC conditioned medium. SB-431542 partially inhibited SLF proliferation that was induced by MSC conditioned medium (Fig. 4G).

FGF2, which is also secreted by MSCs (Dormady et al., 2001; Sensebe et al., 1997), was not included in the cytokine array that we used in this study. Because FGF2 and its receptor, FGF-receptor 1 (FGFR1), are expressed at high levels in the lateral wall of postnatal mouse (Pickles, 2001), we also added the FGFR1 inhibitor SU4984 (Mohammadi et al., 1997) to MSC conditioned medium. This inhibitor did not, however, have

an effect on SLF proliferation in the presence of MSC conditioned medium (Fig. 4G).

DISCUSSION

Inner ear cell culture has been successfully reported in epithelial (Rarey and Patterson, 1989; Achouche et al., 1991; Melichar and Gitter, 1992) and endothelial (Bowman et al., 1985) cells. Recently, cell culture of SLFs has also been established and characterized for type I SLFs in gerbils (Gratton et al., 1996), mice (Suko et al., 2000), and rats (Yian et al., 2006). To date, however, there are no reports on the successful establishment of a concurrent culture of all types of SLFs, which more closely mimics the in vivo condition. In the present study, we attempted to establish such an SLF culture system using isolated cells from mice. Our cultured cells contained spindle-shaped cells, which are morphologically compatible with fibrocytes, and immunocytochemical analysis detected the markers of all four types of SLFs. This novel SLF culture system, which more closely mimics conditions in vivo, may be especially useful in elucidating the effects of a specific condition on the cochlear ion homeostasis.

Many factors are known to affect the differentiation of MSCs. These include soluble growth factors and cytokines (Otto and Lane, 2005; Bowers and Lane, 2007), mechanical stimuli (Lee et al., 2007), surface properties (Guo et al., 2008), and culture conditions (Song et al., 2007). Cell density has been reported to affect cell functions such as proliferation and differentiation (Bitar et al., 2008; Neuhuber et al., 2008). McBeath et al. (2004) have reported that human MSCs plated at lower density are more likely to become osteoblasts, whereas cells plated at higher density are more likely to become adipocytes. In the present study, MSCs did not express markers for SLFs under routine culture conditions. When MSCs were plated on collagen-coated dishes at a lower density, however, a small subgroup of MSCs differentiated into SLF-like cells spontaneously. The collagen coating was likely to have affected MSC differentiation into SLF-like cells, because the SL is made up of fibrocytes embedded in collagen fibrils (Tsuprun and Santi, 1999). Our results also showed that factors secreted by SLFs had the ability to promote MSCs to differentiate into SLF-like cells with no effects on their proliferation. In stem cells or progenitor cells, inhibition of proliferation induces differentiation (Hirose et al., 2006; Jung et al., 2008). Therefore, the lower proliferation of MSCs cultured with SLF conditioned medium may also explain the increase in MSC differentiation into SLF-like cells. The DNA array results showed several genes that were highly expressed in MSCs cultured with SLF conditioned medium. One of these factors, *Wnt8a*, is expressed in rhombomere 4 in embryonic day (E8) mouse (Bouillet et al., 1996) and is the canonical WNT that activates the WNT-β-catenin pathway (Katoh, 2005). *Wnt8* is expressed in the developing hindbrain in chick, mouse, and zebrafish, in which it has been implicated in stabilizing otic fate following induction (Ohyama et al., 2006; Freter et al., 2008). Studies have suggested that canonical Wnt signaling affects MSC proliferation and differentiation (Cho et al., 2000; Boland et al., 2004; De Boer et al., 2004). Further studies are needed to clarify the mechanism by which canonical Wnt signaling regulates MSC proliferation.

Our study clearly demonstrates that conditioned medium from MSCs stimulated SLF proliferation. The cells that were incubated with MSC conditioned medium showed increased expression of vimentin, which is a mesenchymal progenitor marker protein (Rose et al., 2008), whereas the expression of markers of mature SLFs decreased. Immunostaining data from tissue sections of mouse cochlea showed that vimentin was present in SLFs at P0 and that the intensity of labeling decreased after birth. Vimentin is associated with the mitotic apparatus and is related to the induction of cellular DNA synthesis and mitosis. It is involved in the extensive remodeling of cytoskeletal components that is required for mitosis, cell migration, and process outgrowth (Baserga, 1985; Ferrari et al., 1986), so increases in vimentin synthesis are associated with rapidly growing cells. In our study, vimentin immunoreactivity decreased during postnatal development of the SL (Fig. 4C,D). This decreased expression of vimentin in the SL could be indicative of declining mitotic activity across the whole SL, as has been observed in the mouse (Ruben, 1967; Mutai et al., 2009). At P0, vimentin-positive cells did not express markers of mature SLFs, which leads us to speculate that those cells were in an immature state. In the SL of 6-week-old mice, vimentin expression was restricted to a subpopulation of SLFs. SLFs are able to repopulate themselves after noise or drug exposure in the adult mammalian inner ear (Roberson and Rubel, 1994; Hirose and Liberman, 2003; Lang et al., 2003). Immature SLFs or stem cells that reside in the mature SL might explain how SLFs repair or replace themselves. Increased expression of vimentin along with the decreased expression of mature SLF markers that was observed in SLFs cultured with MSC conditioned medium might also be explained by the proliferation of immature SLFs that were stimulated by the factors secreted by the MSCs. Transplanted MSCs might induce the proliferation of such immature SLFs and may thus contribute to the repair of the damaged SL. Whether the stimulated vimentin-positive cells have the ability to differentiate into mature SLFs to restore the damaged SLF network must be clarified in further experiments.

Analyses using DNA and cytokine arrays revealed the involvement of TGF-β signaling in the effect of MSCs on SLFs. TGF-β stimulates or inhibits the growth and differentiation of cells (McCartney-Francis et al., 1998). Reciprocal interactions between the developing otic epithelium and the periotic mesenchymal tissue are critical for normal inner ear morphogenesis. As a secreted protein, TGF-β participates in these interactions in a variety of developing tissues (Massague, 1990; Kingsley, 1994). TGF-β3 is expressed throughout the cochlear epithelium at E13.5–E17.5 (Pelton et al., 1991).

The type II TGF-β receptor (TbRII), which mediates many of the biological responses to TGF-β, is found in the mesenchyme surrounding the inner ear (Wang et al., 1995). TGF-β ligands bind to heteromeric complexes of TbRI and TbRII (Massague, 1998; Shi and Massague, 2003). SB-431542, an inhibitor of TbRI (Laping et al., 2002), blocks the TGF-β-mediated proliferation of a mesenchymal cell line (Matsuyama et al., 2003). In this study, SB-431542 partially inhibited SLF proliferation that was induced by the addition of MSC conditioned medium, suggesting that TGF-β secreted from MSCs contributes to the proliferation of SLFs. Because the transplantation of stem cells, combined with specific growth factors and cytokines, has been thought to have great potential in regenerative medicine, the identification of paracrine factors from MSCs should be helpful in improving the success of MSC transplantation.

The DNA array results in SLFs stimulated with MSC conditioned medium revealed genes with a known role in apoptosis (Table III). Overexpression of the gene encoding *PTTG1*, one of these upregulated genes, decreases UV-induced apoptosis (Lai et al., 2007), and increased expression of *PTTG1* increases cell proliferation (Kakar and Jennes, 1999; Zhang et al., 1999; Hamid et al., 2005). In a similar manner, accelerated proliferation of SLFs induced by the factors secreted by MSCs may result from increased cell proliferation and resistance to apoptosis. In addition, SLFs cultured with or without MSC conditioned medium also showed differential expression of several genes related to extracellular matrix and adhesion molecules (Table III). *Thbs1* and *MMP11*, which were downregulated in SLFs with MSC stimulation, are involved in apoptosis (Friedl et al., 2002) and cell proliferation (Deng et al., 2005), respectively. The effects of these molecules on SLFs should be investigated in a future study. In the 3NP model, rats with injury to the SL had a higher rate of MSC invasion than did those without injury (Kamiya et al., 2007). Our results here show that factors secreted by MSCs induced SLF proliferation. Thus we speculate that the transplanted MSCs in the injured SL might promote SLFs to regenerate, leading to hearing recovery. In addition, we found that SLF conditioned medium promoted the transdifferentiation of MSCs into SLF-like cells. Whether transplanted MSCs in vivo have this ability to transdifferentiate into SLF-like cells must be determined in the future. MSCs expressed the gap junction protein Cx31, which is related to hearing loss (Mhatre et al., 2003), regardless of exposure to SLF conditioned medium (data not shown). In the injured SL, transplanted MSCs protrude toward neighboring fibrocytes and express the cochlear gap junction protein connexin 26 (Kamiya et al., 2007). Gap junctions between cochlear fibrocytes play an important role in the cochlear potassium recycling system, and a disrupted gap junction network, which occurs with the loss of SLFs, is thought to be one of the main causes of hearing loss (Lopez-Bigas et al., 2002). Taken together, these data suggest that the expression of gap junctions on MSCs is likely to play a role in reorganizing the gap junction network that occurs with the loss of SLFs.

CONCLUSIONS

Our results suggest that two mechanisms of hearing recovery occur in the damaged SL after transplantation of MSCs into the inner ear. One is that the transplanted MSCs transdifferentiate into SLF-like cells that compensate for the lost SLFs. The other is that the transplanted MSCs stimulate the proliferation and regeneration of the host SLFs. In this study, several candidate molecules that might be involved in these mechanisms were detected, and the role of TGF-β signaling in the proliferation of SLFs was verified. Further elucidation of key molecules in these mechanisms may lead to the establishment of a new therapeutic approach for sensorineural hearing loss.

ACKNOWLEDGMENTS

We thank Susumu Nakagawa for technical assistance.

REFERENCES

Achouche J, Wu AH, Liu DS, Huy PTB. 1991. Primary culture of strial marginal cells of guinea-pig cochlea—growth, morphological features, and characterization. Ann Otol Rhinol Laryngol 100:999–1006.

Baserga R. 1985. The biology of cell reproduction. Cambridge, MA: Harvard University Press. 251 p.

Benzeev A. 1985. Cell-density and cell shape-related regulation of vimentin and cytokeratin synthesis-inhibition of vimentin synthesis and appearance of a new 45-kD cytokeratin in dense epithelial-cell cultures. Exp Cell Res 157:520–532.

Bitar M, Brown RA, Salih V, Kidane AG, Knowles JC, Nazhat SN. 2008. Effect of cell density on osteoblastic differentiation and matrix degradation of biomimetic dense collagen scaffolds. Biomacromolecules 9:129–135.

Boland GM, Perkins G, Hall DJ, Tuan RS. 2004. Wnt 3a promotes proliferation and suppresses osteogenic differentiation of adult human mesenchymal stem cells. J Cell Biochem 93:1210–1230.

Bouillet P, OuladAbdelghani M, Ward SJ, Bronner S, Chambon P, Dolle P. 1996. A new mouse member of the Wnt gene family, mWnt-8, is expressed during early embryogenesis and is ectopically induced by retinoic acid. Mech Dev 58:141–152.

Bowers RR, Lane MD. 2007. A role for bone morphogenetic protein-4 in adipocyte development. Cell Cycle 6:385–389.

Bowman PD, Rarey K, Rogers C, Goldstein GW. 1985. Primary culture of capillary endothelial-cells from the spiral ligament and stria vasculars of bovine inner ear retention of several endothelial-cell properties in vitro. Cell Tissue Res 241:479–486.

Cho HH, Kim SH, Kim YG, Kim YC, Koller H, Camblor MA, Hong SB. 2000. Synthesis and characterization of gallosilicate molecular sieves with high gallium contents: examples of structure direction exerted by gallium. Chem Mater 12:2292–2300.

De Boer J, Wang HJ, Van Blitterswijk C. 2004. Effects of Wnt signaling on proliferation and differentiation of human mesenchymal stem cells. Tissue Eng 10:393–401.

Delprat B, Ruel J, Guitton MJ, Hamard G, Lenoir M, Pujol R, Puel JL, Brabet P, Hamel CP. 2005. Deafness and cochlear fibrocyte alterations in mice deficient for the inner ear protein otospiralin. Mol Cell Biol 25:847–853.

Deng H, Guo RF, Li WM, Zhao M, Lu YY. 2005. Matrix metalloproteinase 11 depletion inhibits cell proliferation in gastric cancer cells. Biochem Biophys Res Commun 326:274–281.

Dormady SP, Bashayan O, Dougherty R, Zhang XM, Basch RS. 2001. Immortalized multipotential mesenchymal cells and the hematopoietic microenvironment. J Hematother Stem Cell Res 10:125–140.

Ferrari S, Battini R, Kaczmarek L, Rittling S, Calabretta B, de Riel JK, Philiponis V, Wei JF, Baserga R. 1986. Coding sequence and growth regulation of the human vimentin gene. Mol Cell Biol 6:3614–3620.

Freter S, Muta Y, Mak S-S, Rinkwitz S, Ladher RK. 2008. Progressive restriction of otic fate: the role of FGF and Wnt in resolving inner ear potential. Development 135:3415–3424.

Friedl P, Vischer P, Freyberg MA. 2002. The role of thrombospondin-1 in apoptosis. Cell Mol Life Sci 59:1347–1357.

Gratton MA, Schulte BA, Hazen-Martin DJ. 1996. Characterization and development of an inner ear type I fibrocyte cell culture. Hear Res 99:71–78.

Guo L, Kawazoe N, Fan Y, Ito Y, Tanaka J, Tateishi T, Zhang X, Chen G. 2008. Chondrogenic differentiation of human mesenchymal stem cells on photoreactive polymer-modified surfaces. Biomaterials 29:23–32.

Hamid T, Malik MT, Kakar SS. 2005. Ectopic expression of PTTGI/securin promotes tumorigenesis in human embryonic kidney cells. Mol Cancer 4.

Hequembourg S, Liberman MC. 2001. Spiral ligament pathology: a major aspect of age-related cochlear degeneration in C57BL/6 mice. J Assoc Res Otol 2:118–129.

Hirose K, Liberman MC. 2003. Lateral wall histopathology and endocochlear potential in the noise-damaged mouse cochlea. J Assoc Res Otol 4:339–352.

Hirose M, Hashimoto H, Iga J, Shintani N, Nakanishi M, Arakawa N, Shimada T, Baba A. 2006. Inhibition of self-renewal and induction of neural differentiation by PACAP in neural progenitor cells. Vip Pacap Rel Peptides Gene Ther 1070:342–347.

Hoya N, Okamoto Y, Kamiya K, Fujii M, Matsunaga T. 2004. A novel animal model of acute cochlear mitochondrial dysfunction. Neuroreport 15:1597–1600.

Huang SS, Huang JS. 2005. TGF-beta control of cell proliferation. J Cell Biochem 96:447–462.

Islam MQ, Meirelles LD, Nardi NB, Magnusson P, Islam K. 2006. Polyethylene glycol-mediated fusion between primary mouse mesenchymal stem cells and mouse fibroblasts generates hybrid cells with increased proliferation and altered differentiation. Stem Cells Dev 15:905–919.

Jung GA, Yoon JY, Moon BS, Yang DH, Kim HY, Lee SH, Bryja V, Arenas E, Choi KY. 2008. Valproic acid induces differentiation and inhibition of proliferation in neural progenitor cells via the beta-catenin-Ras-ERK-p21(Cip/WAF1) pathway. BMC Cell Biol 9.

Kakar SS, Jennes L. 1999. Molecular cloning and characterization of the tumor transforming gene (TUTR1): a novel gene in human tumorigenesis. Cytogenet Cell Genet 84:211–216.

Kamiya K, Fujinami Y, Hoya N, Okamoto Y, Kouike H, Komatsuzaki R, Kusano R, Nakagawa S, Satoh H, Fujii M, Matsunaga T. 2007. Mesenchymal stem cell transplantation accelerates hearing recovery through the repair of injured cochlear fibrocytes. Am J Pathol 171:214–226.

Katoh M. 2005. Comparative genomics on Wnt8a and Wnt8b genes. Int J Oncol 26:1129–1133.

Kingsley DM. 1994. The TGF-beta superfamily—new menbers, new receptors, and new genetic tests of function in different organisms. Genes Dev 8:133–146.

Kuijpers W, Tonnaer EL, Peters TA, Ramaekers FC. 1992. Developmentally-regulated coexpression of vimentin and cytokeratins in the rat inner ear. Hear Res 62:1–10.

Lai YQ, Xin DQ, Bai JH, Mao ZB, Na YQ. 2007. The important anti-apoptotic role and its regulation mechanism of PTTG1 in UV-induced apoptosis. J Biochem Mol Biol 40:966–972.

Lang H, Schulte BA, Schmiedt RA. 2003. Effects of chronic furosemide treatment and age on cell division in the adult gerbil inner ear. J Assoc Res Otol 4:164–175.

Laping NJ, Grygielko E, Mathur A, Butter S, Bomberger J, Tweed C, Martin W, Fornwald J, Lehr R, Harling J, Gaster L, Callahan JF, Olson BA. 2002. Inhibition of transforming growth factor (TGF)-beta 1-induced extracellular matrix with a novel inhibitor of the TGF-beta type I receptor kinase activity: SB-431542. Mol Pharmacol 62:58–64.

Lee IC, Wang JH, Lee YT, Young TH. 2007. The differentiation of mesenchymal stem cells by mechanical stress or/and co-culture system. Biochem Biophys Res Commun 352:147–152.

Lopez-Bigas N, Arbones ML, Estivill X, Simonneau L. 2002. Expression profiles of the connexin genes, Gjb1 and Gjb3, in the developing mouse cochlea. Gene Express Pattern 2:113–117.

Massague J. 1990. The transforming growth factor beta family. Annu Rev Cell Biol 6:597–641.

Massague J. 1998. TGF-beta signal transduction. In: Richardson CC, editor. Annu Rev Biochem. p 753–791.

Matsuyama S, Iwadate M, Kondo M, Saitoh M, Hanyu A, Shimizu K, Aburatani H, Mishima HK, Imamura T, Miyazono K, Miyazawa K. 2003. SB-431542 and Gleevec inhibit transforming growth factor-13-induced proliferation of human osteosarcoma. Cancer Res 63:7791–7798.

McBeath R, Pirone DM, Nelson CM, Bhadriraju K, Chen CS. 2004. Cell shape, cytoskeletal tension, and RhoA regulate stem cell lineage commitment. Dev Cell 6:483–495.

McCartney-Francis NL, Frazier-Jessen M, Wahl SM. 1998. TGF-beta: a balancing act. Int Rev Immunol 16:553–580.

Melichar I, Gitter AH. 1992. Ultrastructure of cultured marginal cells of the guinea pig cochlea. Acta Otolaryngol 112:762–766.

Mhatre AN, Weld E, Lalwani AK. 2003. Mutation analysis of connexin 31 (GJB3) in sporadic non-syndromic hearing impairment. Clin Genet 63:154–159.

Minowa O, Ikeda K, Sugitani Y, Oshima T, Nakai S, Katori Y, Suzuki M, Furukawa M, Kawase T, Zheng Y, Ogura M, Asada Y, Watanabe K, Yamanaka H, Gotoh S, Nishi-Takeshima M, Sugimoto T, Kikuchi T, Takasaka T, Noda T. 1999. Altered cochlear fibrocytes in a mouse model of DFN3 nonsyndromic deafness. Science 285:1408–1411.

Mizutari K, Nakagawa S, Mutai H, Fujii M, Ogawa K, Matsunaga T. 2011. Late-phase recovery in the cochlear lateral wall following severe degeneration by acute energy failure. Brain Res 1419:1–11.

Mohammadi M, McMahon G, Sun L, Tang C, Hirth P, Yeh BK, Hubbard SR, Schlessinger J. 1997. Structures of the tyrosine kinase domain of fibroblast growth factor receptor in complex with inhibitors. Science 276:955–960.

Mutai H, Nagashima R, Fujii M, Matsunaga T. 2009. Mitotic activity and specification of fibrocyte subtypes in the developing rat cochlear lateral wall. Neuroscience 163:1255–1263.

Neuhuber B, Swanger SA, Howard L, Mackay A, Fischer I. 2008. Effects of plating density and culture time on bone marrow stromal cell characteristics. Exp Hematol 36:1176–1185.

Ohyama T, Mohamed OA, Taketo MM, Dufort D, Groves AK. 2006. Wnt signals mediate a fate decision between otic placode and epidermis. Development 133:865–875.

Okamoto Y, Hoya N, Kamiya K, Fujii M, Ogawa K, Matsunaga T. 2005. Permanent threshold shift caused by acute cochlear mitochondrial dysfunction is primarily mediated by degeneration of the lateral wall of the cochlea. Audiol Neurootol 10:220–233.

Otto TC, Lane MD. 2005. Adipose development: from stem cell to adipocyte. Crit Rev Biochem Mol Biol 40:229–242.

Pelton RW, Saxena B, Jones M, Moses HL, Gold LI. 1991. Immunohistochemical localization of TGF-beta1, TGF-beta2, and TGF-beta 3 in the mouse embryo expression patterns suggest mutiple roles during embryonic development. J Cell Biol 115:1091–1105.

Pickles JO. 2001. The expression of fibroblast growth factors and their receptors in the embryonic and neonatal mouse inner ear. Hear Res 155:54–62.

Rarey KE, Patterson K. 1989. Estabilishment of innerear epithelial cell culture—isolation, growth and characterization. Hear Res 38:277–287.

Roberson DW, Rubel EW. 1994. Cell division in the gerbil cochlea after acoustic trauma. Am J Otol 15:28–34.

Rose RA, Jiang H, Wang X, Helke S, Tsoporis JN, Gong N, Keating SCJ, Parker TG, Backx PH, Keating A. 2008. Bone marrow-derived mesenchymal stromal cells express cardiac-specific markers, retain the stromal phenotype, and do not become functional cardiomyocytes in vitro. Stem Cells 26:2884–2892.

Ruben R. 1967. Development of the inner ear of the mouse: a radioautographic study of terminal mitoses. Acta Otolaryngol Suppl 220:1–44.

Schulte BA, Steel KP. 1994. Expression of alpha-subunit and beta-subunit isoforms of Na,K-ATPase in the mouse inner-ear and changes with mutations at the W-V or Sld loci. Hear Res 78:65–76.

Sensebe L, Deschaseaux M, Li J, Herve P, Charbord P. 1997. The broad spectrum of cytokine gene expression by myoid cells from the human marrow microenvironment. Stem Cells 15:133–143.

Shi YG, Massague J. 2003. Mechanisms of TGF-beta signaling from cell membrane to the nucleus. Cell 113:685–700.

Song SJ, Jeon O, Yang HS, Ran DK, Kim BS. 2007. Effects of culture conditions on osteogenic differentiation in human mesenchymal stem cells. J Microbiol Biotechnol 17:1113–1119.

Spicer SS, Schulte BA. 1991. Differentiation of inner-ear fibrocyties according to their ion-transport related activity. Hear Res 56:53–64.

Spicer SS, Schulte BA. 1996. The fine structure of spiral ligament cells relates to ion return to the stria and varies with place-frequency. Hear Res 100:80–100.

Spicer SS, Schulte BA. 2002. Spiral ligament pathology in quiet-aged gerbils. Hear Res 172:172–185.

Suko T, Ichimiya I, Yoshida K, Suzuki M, Mogi G. 2000. Classification and culture of spiral-ligament fibrocytes from mice. Hear Res 140:137–144.

Takahashi T, Kimura RS. 1970. The ultrastructure of the spiral ligament in the Rhesus monkey. Acta Otolaryngol 69:46–60.

Tsuprun V, Santi P. 1999. Ultrastructure and immunohistochemical identification of the extracellular matrix of the chinchilla cochlea. Hear Res 129:35–49.

Wang YQ, Sizeland A, Wang XF, Sassoon D. 1995. Restricted expression of type-II TGF-beta receptor in murine embryonic development suggest a central role in tissue modeling and CNS patterning. Mech Dev 52:275–289.

Wangemann P. 2002. K^+ cycling and the endocochlear potential. Hear Res 165:1–9.

Weber PC, Cunningham CD, Schulte BA. 2001. Potassium recycling pathways in the human cochlea. Laryngoscope 111:1156–1165.

Yian C, Moon SK, Jin SJ, Webster P, Rhim JS, Andalibi A, Lim DJ. 2006. Characterization of rat spiral ligament cell line immortalized by adenovirus 12-simian virus 40 hybrid virus. Ann Otol Rhinol Laryngol 115:930–938.

Zhang X, Horwitz GA, Prezant TR, Valentini A, Nakashima M, Bronstein MD, Melmed S. 1999. Structure, expression, and function of human pituitary tumor-transforming gene (PTTG). Mol Endocrinol 13:156–166.

CLINICAL GENETICS An International Journal of Genetics, Molecular and Personalized Medicine

Clin Genet 2012: 82: 425–432
Printed in Singapore. All rights reserved

CLINICAL GENETICS
doi: 10.1111/j.1399-0004.2012.01897.x

Original Article

A prevalent founder mutation and genotype–phenotype correlations of *OTOF* in Japanese patients with auditory neuropathy

T Matsunaga[a], H Mutai[a], S Kunishima[b], K Namba[a], N Morimoto[c], Y Shinjo[d], Y Arimoto[e], Y Kataoka[f], T Shintani[g], N Morita[h], T Sugiuchi[i], S Masuda[j], A Nakano[e], H Taiji[c] and K Kaga[d]

[a]Laboratory of Auditory Disorders, National Institute of Sensory Organs, National Tokyo Medical Center, Tokyo, Japan, [b]Department of Advanced Diagnosis, Clinical Research Center, National Hospital Organization Nagoya Medical Center, Nagoya, Japan, [c]Department of Otorhinolaryngology, National Center for Child Health and Development, Tokyo, Japan, [d]National Institute of Sensory Organs, National Hospital Organization Tokyo Medical Center, Tokyo, Japan, [e]Division of Otorhinolaryngology, Chiba Children's Hospital, Chiba, Japan, [f]Department of Otolaryngology, Head and Neck Surgery, Okayama University Postgraduate School of Medicine, Dentistry and Pharmaceutical Science, Okayama, Japan, [g]Department of Otolaryngology, Sapporo Medical University School of Medicine, Sapporo, Japan, [h]Department of Otolaryngology, Teikyo University School of Medicine, Tokyo, Japan, [i]Department of Otolaryngology, Kanto Rosai Hospital, Kawasaki, Japan, and [j]Department of Otorhinolaryngology, Institute for Clinical Research, National Mie Hospital, Tsu, Japan

Key words: auditory neuropathy – genotype–phenotype correlation – mutation – non-syndromic hearing loss – *OTOF*

Corresponding author: Tatsuo Matsunaga MD, PhD, Laboratory of Auditory Disorders and Department of Otolaryngology, National Institute of Sensory Organs, National Tokyo Medical Center, 2-5-1 Higashigaoka, Meguro, Tokyo 152-8902, Japan.

Matsunaga T, Mutai H, Kunishima S, Namba K, Morimoto N, Shinjo Y, Arimoto Y, Kataoka Y, Shintani T, Morita N, Sugiuchi T, Masuda S, Nakano A, Taiji H, Kaga K. A prevalent founder mutation and genotype–phenotype correlations of *OTOF* in Japanese patients with auditory neuropathy.
Clin Genet 2012: 82: 425–432. © John Wiley & Sons A/S, 2012

Auditory neuropathy is a hearing disorder characterized by normal outer hair cell function and abnormal neural conduction of the auditory pathway. Aetiology and clinical presentation of congenital or early-onset auditory neuropathy are heterogeneous, and their correlations are not well understood. Genetic backgrounds and associated phenotypes of congenital or early-onset auditory neuropathy were investigated by systematically screening a cohort of 23 patients from unrelated Japanese families. Of the 23 patients, 13 (56.5%) had biallelic mutations in *OTOF*, whereas little or no association was detected with *GJB2* or *PJVK*, respectively. Nine different mutations of *OTOF* were detected, and seven of them were novel. p.R1939Q, which was previously reported in one family in the United States, was found in 13 of the 23 patients (56.5%), and a founder effect was determined for this mutation. p.R1939Q homozygotes and compound heterozygotes of p.R1939Q and truncating mutations or a putative splice site mutation presented with stable, and severe-to-profound hearing loss with a flat or gently sloping audiogram, whereas patients who had non-truncating mutations except for p.R1939Q presented with moderate hearing loss with a steeply sloping, gently sloping or flat audiogram, or temperature-sensitive auditory neuropathy. These results support the clinical significance of comprehensive mutation screening for auditory neuropathy.

Conflict of interest

The authors declare no conflict of interest.

Tel.: +81 3 3411 0111;
fax: +81 3 3412 9811;
e-mail:
matsunagatatsuo@kankakuki.go.jp

Received 28 February 2012, revised and accepted for publication 6 April 2012

Auditory neuropathy (AN) is a hearing disorder characterized by normal outer hair cell function, as revealed by the presence of otoacoustic emissions (OAE) or cochlear microphonics, and abnormal neural conduction of the auditory pathway, as revealed by the absence or severe abnormality of auditory brainstem responses (ABR) (1). Hearing disorders having the same characteristics have also been reported as auditory nerve disease in adult cases (2). Individuals with AN invariably have difficulties in understanding speech (3), and approximately 10% of infants diagnosed with profound hearing loss have AN (3, 4).

About 50% of subjects with congenital or early-onset AN have risk factors such as perinatal hypoxia, whereas the remaining 50% of subjects are likely to have a genetic factor (3, 5). To date, four loci responsible for non-syndromic AN have been mapped: DFNB9 caused by *OTOF* mutation and DFNB59 caused by *PJVK* mutation, both of which are responsible for autosomal recessive AN; AUNA1 caused by DIAPH3 mutation, which is responsible for autosomal dominant AN; and AUNX1, which is responsible for X-linked AN (6–9). Mutations in *OTOF*, which contains 50 exons and encodes short and long isoforms of otoferlin (10), are the most frequent mutations associated with AN with various frequency depending on the population studied (11–15). Most *OTOF* genotypes have been associated with stable, severe-to-profound hearing loss with only a few exceptions (11–20). Studies of genetic backgrounds and clinical phenotypes in various populations will extend our knowledge of genotype–phenotype correlations and may help in the management and treatment of AN.

Materials and methods

Subjects

We enrolled 23 index patients of unrelated Japanese families with congenital or early-onset AN. Diagnosis of hearing loss was made by age 2 in all patients except for one, who had mild hearing loss diagnosed at age 9. All patients had non-syndromic AN in both ears, and they were collected from all over Japan as part of a multicentre study of AN. Patients with hearing loss of possible environmental risk factors for AN such as neonatal hypoxia or jaundice were excluded. With regard to the family history, one patient had a brother having congenital AN and all others were simplex. DNA samples and medical information were obtained from each proband and, if possible, parents and siblings. For DNA samples, 2 parents, 1 parent, no parent, and 1 sibling were available in 10 families, 4 families, 9 families, and 1 family, respectively. None of parents of 23 index patients complained of hearing loss by clinical interview. For the normal-hearing control, 189 subjects who had normal hearing by pure-tone audiometry were used. This study was approved by the institutional ethics review board at the National Tokyo Medical Center. Written informed consent was obtained from all the subjects included in the study or their parents.

Genetic analysis

DNA was extracted from peripheral blood by standard procedures. Genetic analysis for mutations in *GJB2* and for A1555G and A3243G mitochondrial DNA mutations were conducted in all patients according to published methods (21, 22). Mutation screening of *OTOF* was performed by bidirectional sequencing of amplicons generated by PCR amplification of each exon (exons 1–50) and splice sites using an ABI 3730 Genetic Analyzer (Applied Biosystems, Foster City, CA). Primer sequences for *OTOF* are listed in Table S1, supporting information. Mutation nomenclature is based on genomic DNA sequence (GenBank accession number NG_009937.1), with the A of the translation initiation codon considered as +1. The nucleotide conservation between mammalian species was evaluated by ClustalW (http://www.ebi.ac.uk/Tools/msa/clustalw2/).

To determine whether the prevalent p.R1939Q alleles are derived from a common founder, we conducted haplotype analysis. We genotyped single nucleotide polymorphisms (SNPs) with a minor allele frequency of >0.3 in the Japanese population and a microsatellite marker (D2S2350) spanning the *OTOF* locus and nearby genes on an ABI Genetic Analyzer 310 and Genescan 3.7 software (Applied Biosystems). Forty-four SNPs and the D2S2350 microsatellite marker in the vicinity of the mutation were genotyped in 11 AN patients who had p.R1939Q and in a part of their parents.

In six patients who did not have any mutations in *OTOF* and *GJB2* and three patients who were heterozygous for *OTOF* mutation without any mutations in *GJB2*, all coding exons and splice sites of *PJVK* were sequenced. Primer sequences were designed based on the reference sequence of *PJVK* (GenBank accession number NG_012186) and are listed in Table S2. Novelty of mutations and non-pathogenic variants found in the present study were examined in EVS (http://evs.gs.washington.edu/EVS/) and dbSNP

(http://www.ncbi.nlm.nih.gov/snp). The effect of an amino acid substitution was predicted using PolyPhen-2 software (http://genetics.bwh.harvard.edu/pph2/) and NNSPLICE 0.9 version (Berkley Drosophila Genome Project, http://www.fruitfly.org/seq_tools/splice.html) for the splice sites. The effect of p.D1842N was also analysed by modelling the three-dimensional structure of otoferlin using SWISS-MODEL (http://swissmodel.expasy.org/) (23).

Clinical examination and data analysis

Audiological tests included otoscopic examination and pure-tone audiometry with a diagnostic audiometer in a soundproof room following International Standards Organization standards. On the basis of pure-tone air-conduction thresholds, the degree of hearing loss was determined by the better ear pure-tone average across the frequencies 0.5, 1, 2, and 4 kHz, and it was classified as mild (20–40 dB), moderate (41–70 dB), severe (71–95 dB), or profound (>95 dB) according to the recommendations for the description of audiological data by the Hereditary Hearing Loss Homepage (http://hereditaryhearingloss.org).

Results

Genetic findings

Of 23 patients with a diagnosis of congenital or early-onset AN, 13 (56.5%) carried two pathogenic *OTOF* alleles, and 3 patients (13.0%) carried one pathogenic allele (Fig. 1: inner circle). In summary, 70% of the patients had pathogenic *OTOF* alleles. Results of genotyping of the detected pathogenic *OTOF* alleles in 13 families carrying two pathogenic *OTOF* alleles (10 families in which two parents were examined and 3 families in which one parent was examined) were compatible with autosomal recessive inheritance in all these families. *OTOF* mutations consisted of three missense mutations, one frameshift mutation, two nonsense mutations, one non-stop mutation, and two putative splice site mutations (Tables 1 and 2). p.R1939Q was previously reported as a mutation and IVS47-2A>G was previously reported in dbSNP. Other seven *OTOF* mutations were novel. p.R1939Q was found in 43.5% of all alleles. We also identified 16 non-pathogenic *OTOF* variants, of which only p.P1697P was novel (Table 1). This variant did not change the score of splice site prediction. The location of each mutation in *OTOF* and the evolutionary conservation of the amino acids or nucleotides affected by the missense and putative splice site mutations are shown in Fig. 2a,b. The frequency of different *OTOF* genotypes is summarized in Fig. 1 (middle circle); 56.5% of the patients had p.R1939Q. In contrast, mutations other than p.R1939Q were confined to individual families. Previously, p.R1939Q was reported in one family with AN in the United States (19), and a different mutation in the same codon (p.R1939W) was reported in another family (16). Screening for the mutation

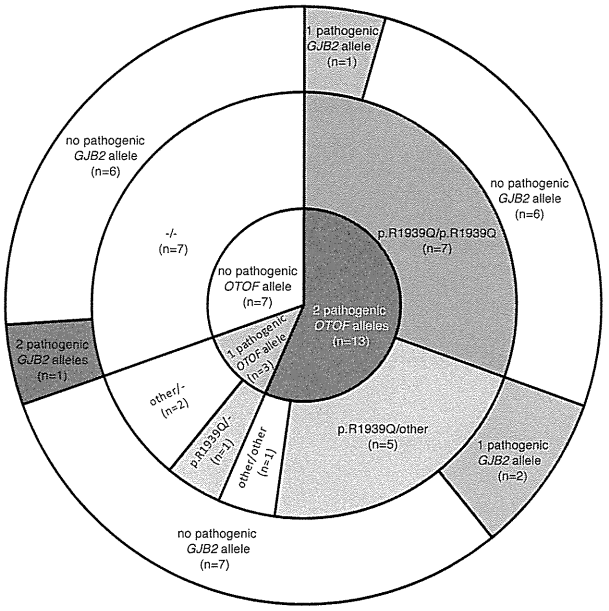

Fig. 1. Genetic backgrounds and frequency of different *OTOF* alleles in patients with congenital or early-onset auditory neuropathy (AN). (a) Distribution of patients carrying different pathogenic *OTOF* alleles (inner circle), *OTOF* genotypes (middle circle), and *GJB2* genotypes (outer circle). p.R1939Q indicates *OTOF* allele with p.R1939Q mutation; other indicates pathogenic *OTOF* alleles except for p.R1939Q allele; *n* indicates number of patients.

in 189 control subjects with normal hearing revealed only one heterozygous carrier. This mutation was predicted to be probably damaging variant according to PolyPhen-2.

The novel missense mutation p.D1842N was identified in a heterozygote without accompanying pathogenic alleles (patient 15). The mutation was predicted to be probably damaging variant according to PolyPhen-2. D1842 is located within the C2F domain, which is one of six calcium-binding modules (C2 domains) in otoferlin that are indispensable for otoferlin function. The predicted three-dimensional protein structure suggested that this mutation generates a repulsive force on calcium ions, resulting in reduced otoferlin activity (Fig. 3a–c). Another novel missense mutation, p.G541S, was identified as homozygous in a patient with parental consanguinity (patient 13). This mutation was predicted to be probably damaging variant according to PolyPhen-2 and involves a change from a non-polar residue to a polar residue in the C2C domain.

The c.1946-1965 del20 frameshift mutation truncates otoferlin at S648, causing a change in stop codon that adds six residues to the C terminus. Two nonsense mutations, p.Y474X and p.Y1822X, also truncate otoferlin. It is possible that these mutations trigger the nonsense-mediated decay response, by which aberrant mRNA is eliminated before translation (24). Even if the truncated proteins were produced, they would not function well because the mutations in c.1946-1965 del20, p.Y474X, and p.Y1822X disrupt three